Plant Stress 14 (2024) 100697

Contents lists available at ScienceDirect

Plant Stress

journal homepage: www.sciencedirect.com/journal/plant-stress

Molecular mechanisms underlying tree host-pathogen interactions under drought stress and subsequent rewatering in *Eucalyptus grandis*

Demissew Tesfaye Teshome [a], Godfrey Elijah Zharare [b], Raphael Ployet [c], Sanushka Naidoo [a,*]

[a] Department of Biochemistry, Genetics and Microbiology, Forestry and Agricultural Biotechnology Institute, University of Pretoria, Lynwood Road, Pretoria, 0028, South Africa
[b] Department of Agriculture, University of Zululand, 1 Main Road Vulindlela, KwaDlangezwa, 3886, South Africa
[c] Biosciences Division, Oak Ridge National Laboratory, 1 Bethel Valley Rd, Oak Ridge, TN 37831, USA

ARTICLE INFO

Keywords:
Combined stress
Water stress
Forest tree
Fungal pathogen
Drought recovery

ABSTRACT

Abiotic stresses such as drought change plant-pathogen interactions by affecting both hosts and pathogens. Here, we aimed to unravel the molecular mechanisms underlying forest tree-pathogen interactions under drought stress and subsequent rewatering. We conducted glasshouse experiments involving infection by the stem canker-causing fungal pathogen *Chrysoporthe austroafricana* under drought stress and rewatering in *Eucalyptus grandis* and investigated host and pathogen transcriptomic changes using RNA-seq data from our current combined stress experiment as well as previous single stress studies. We found that mild drought stress enhances disease progression while, upon rewatering, pathogen infection delays recovery of leaf stomatal conductance. Transcriptomic changes in the host support increased susceptibility to the pathogen while the *in planta* fungal transcriptome suggests prioritization of survival in the drought-stressed host. Upon rewatering, changes in the host transcriptome suggest allocation of resources to stress responses at the expense of growth and carbohydrate storage while that of the pathogen indicate downregulation of some fungal metabolic pathways potentially because the pathogen takes advantage of changes in the host. Our study identified key molecular processes and genes that provide mechanistic insights into tree-pathogen interactions under abiotic stresses. This enables prediction of tree resilience under a changing climate and contributes towards future tree health improvement endeavours.

1. Introduction

Plants are vulnerable to combinations of multiple biotic and abiotic stresses. In the case of trees, this may include several cycles of exposure to and recovery from abiotic stresses such as drought co-occurring with or triggering pathogen attacks. Under combined stress, the oscillations in the abiotic stressors could affect both the host plants and biotic stressors (Teshome et al., 2020; Zarattini et al., 2021). Some of the molecular changes in plants due to combined stress have been observed to be different from those due to exposure to any of the single stresses (Prasch & Sonnewald, 2013; Gupta et al., 2016). Hence, extrapolating responses to multiple stressors from single stress experiments performed in a controlled environment may not capture the complexity of the regulations involved, especially in perennial plants. This implies that our current knowledge on the resistance/tolerance of plants to combined biotic and abiotic stresses, mainly based on single stress studies, may not be sufficient to predict what could happen under future climate. For example, the effectiveness of a gene conferring resistance against *Xanthomonas oryzae* in rice (*Oryza sativa*) increased at higher temperature, while that of other resistance genes decreased (Webb et al., 2010). Thus, as the exposure of plants to multiple biotic and abiotic stresses will likely increase with changing climate-related droughts and heatwaves, among others, more emphasis should be given to understanding their responses to combined stress (Mittler, 2006; Suzuki et al., 2014; Teshome et al., 2020).

Although studies focusing on the physiological changes of forest trees in response to combined stresses have been increasing in recent years (reviewed in Teshome et al., 2020; Gomez-Gallego et al., 2022; Santos et al., 2024), investigations of the molecular mechanisms underlying these changes are rare in the literature (Ghosh et al., 2022). Model systems in which the responses of plants to individual biotic and abiotic stresses are well-investigated could be used to enhance our

---

* Corresponding author.
E-mail address: sanushka.naidoo@up.ac.za (S. Naidoo).

https://doi.org/10.1016/j.stress.2024.100697
Received 10 June 2024; Received in revised form 23 November 2024; Accepted 1 December 2024

understanding of plant responses to combined stress conditions. This includes the interaction between the fungal pathogen *Chrysoporthe austroafricana* and the economically important perennial biomass crop *Eucalyptus grandis*, which has been established as a model pathosystem to explore the response of trees to fungal pathogens (Naidoo et al., 2013; Mangwanda et al., 2015; 2016; Zwart et al., 2017).

The molecular responses of *E. grandis* to *C. austroafricana* infection have been investigated using the *E. grandis* clonal genotypes, ZG14 and TAG5 (Mondi, South Africa), which were found to be susceptible and moderately resistant to *C. austroafricana*, respectively (Van Heerden et al., 2005). Defense against this pathogen mainly involves phytohormones such as salicylic acid (SA), gibberellic acid (GA), and jasmonic acid (JA) (Naidoo et al., 2013; Mangwanda et al., 2015; Zwart et al., 2017). Higher SA and lower JA concentrations, conforming to the SA-JA mutual antagonism established in *E. grandis* (Naidoo et al., 2013), have been observed at the basal level in TAG5 compared to that in ZG14 (Mangwanda et al., 2015). In the early stages of pathogen infection, both SA and GA concentration decreased in TAG5 but not in ZG14 (Mangwanda et al., 2015). In line with these changes, transcriptomic and proteomic studies revealed differences in the expression of key genes governing the biosynthesis and signalling of these phytohormones in both the host and the pathogen (Mangwanda et al., 2015; 2016; Zwart et al., 2017) showing that these signalling pathways are critical in response to pathogen infection in *Eucalyptus*.

On the other hand, drought stress has been shown to activate the abscisic acid (ABA) signalling pathways in many herbaceous (Yoshida et al., 2014; Kuromori et al., 2018) and woody species, including *E. grandis* (Teshome et al., 2023). ABA is known to have a concentration-dependent antagonism with both JA/ET and SA signalling pathways (Cao et al., 2011; Robert-Seilaniantz et al., 2011). In *Arabidopsis*, the antagonistic interaction between ABA and SA signalling pathways has been shown to mediate drought-induced susceptibility to *Pseudomonas syringae* (Choudhary and Senthil-Kumar, 2022). The molecular and physiological changes related to recovery from drought was also shown to impact the response of plants to cooccurring or subsequent pathogen attacks by leading to either priming or predisposition (Bostock et al., 2014). For example, infection during recovery from drought stress reduced bacterial reproduction in *Arabidopsis* and improved resistance to *P. syringae* (Gupta & Senthil-Kumar, 2017; Illouz-Eliaz et al., 2023). However, studies focusing on such interactions involving necrotrophic pathogens in forest trees have not yet been reported. Previously, we reported transcriptomic changes including genes involved in defense-related phytohormone signalling pathways during drought stress and recovery in the *E. grandis* genotype, moderately resistant to *C. austroafricana* infection, TAG5 (Teshome et al., 2023), suggesting an impact on resistance to pathogen infection.

In this study, we aimed to unravel the molecular mechanisms underlying drought × disease interaction in a forest tree species using the *E. grandis-C. austroafricana* pathosystem as a model. By monitoring disease progression and exploring the transcriptomic profiles of both the host and the pathogen, we show how tree-pathogen interactions change under drought stress and subsequent rewatering. Our results reveal how host plant immunity changes and the pathogen thrives in its tree host under the different watering conditions. By lending insights into the mechanisms of tree-pathogen interactions under episodes of weather extremes and recovery periods, our study contributes towards a better understanding of the biological processes underlying tree health risks under a changing climate.

2. Materials and methods

2.1. Drought stress/rewatering-pathogen inoculation glasshouse experiment

We conducted a glasshouse experiment involving combined drought stress/rewatering and inoculation by the CMW2113 isolate of the fungal pathogen *Chrysoporthe austroafricana* Gryzenhout & M.J. Wingf. in the *Eucalyptus grandis* W. Hill ex Maiden clone, TAG5 (Fig. 1). The transcriptomic responses to the single stresses of *C. austroafricana* infection and drought as well as rewatering following exposure to the single stress of drought has been previously investigated in this genotype (Mangwanda et al., 2015; Teshome et al., 2023). We transplanted two-year-old ramets into 10 litre pots filled with a 4:2:1 [v/v] mixture of potting mix (Culterra Pty Ltd, South Africa), river sand, and vermiculite and supplemented each pot with 10 g slow-release fertilizer. The plants were acclimatized to glasshouse conditions in three phytotrons which served as blocks in a randomized complete block design. Then, we randomly allocated the pots into water-stressed (WS) and well-watered (WW) treatments. After water had been withheld in the WS pots for 7 days, plants in each of the WW and WS groups were inoculated either with *C. austroafricana* (IN) or sterile agar plugs (mock-inoculated, MI) following previously described procedures (Roux et al., 2003; Mangwanda et al., 2015). For the rewatering (RW) treatments, we randomly selected WS pots exposed to progressive drought (Fig. S1a,b) and rewatered them on day 17 (Fig. 1). The soil water content of pots was monitored gravimetrically and the trees were kept under the same conditions as described in Teshome et al. (2023). Briefly, supplementary light was used to keep the plants under long day conditions of 16 h light and 8 h dark with mean daily minimum and maximum temperatures of 24.15 ± 1.51 °C and 29.27 ± 3.62 °C, respectively.

We measured leaf stomatal conductance (*gs*) and stem lesion length and collected stem samples at different timepoints (Fig. 1). We used AP4 porometer (Delta-T Devices Ltd, Cambridge, UK) to measure *gs* from one fully developed leaf each of two ramets in each of three blocks. Stem samples were destructively harvested from 2 cm length flanking either side of the inoculation point. Samples harvested from two ramets were combined for each of three biological replicates per treatment, flash-frozen in liquid nitrogen, and stored at -80 °C until use. Stem samples for three biological replicates each of four treatments harvested on days 3 and 17 (Fig. 1), respectively representing drought and rewatering periods, were ground into fine powder under frozen conditions and used for RNA sequencing (RNA-seq) at BGI Tech Solutions (Hong Kong) Co., Limited, Hong Kong as described in Teshome et al. (2023). Briefly, total RNA was extracted following a modified cetyl-trimethyl-ammonium-bromide (CTAB) protocol. Then, poly-A containing mRNA molecules were selected. This was followed by strand specific cDNA library construction and Illumina sequencing (Illumina, San Diego, CA, USA).

2.2. RNA-seq data pre-processing, differential expression, gene ontology, and transcription factor enrichment analyses

RNA-seq data from the current and previous studies (Mangwanda et al., 2015; 2016; Teshome et al., 2023) were pre-processed as described in Teshome et al. (2023). Briefly, after quality assessment and trimming, aligning the RNA-seq data to the concatenated reference genomes of *E. grandis* (Myburg et al., 2014) and *C. austroafricana* (Wingfield et al., 2015) was followed by transcript quantification. The outputs were imported into the R package DESeq2 to summarize into a transcripts per million matrix and compute differential expression (DE) of genes (Methods S1).

For the rewatering treatments, we computed DE by comparing the WWIN, RWMI, and RWIN treatments with the WWMI control to identify differentially expressed genes (DEGs, Log_2 fold change (L2FC) $> |0.5|$, adjusted P value < 0.05) for the single stress of pathogen infection (PI), recovery from the single stress of drought (RD), and recovery from the combined stresses of drought and pathogen infection (RDPI), respectively. Venn intersection analysis was conducted to identify up- and downregulated genes unique to or shared among PI, RD, and RDPI. Gene ontology biological processes (GO) enrichment was analyzed in these sets of DEGs. We took a selection of specific genes based on previous studies and the co-expression network analysis in this manuscript and

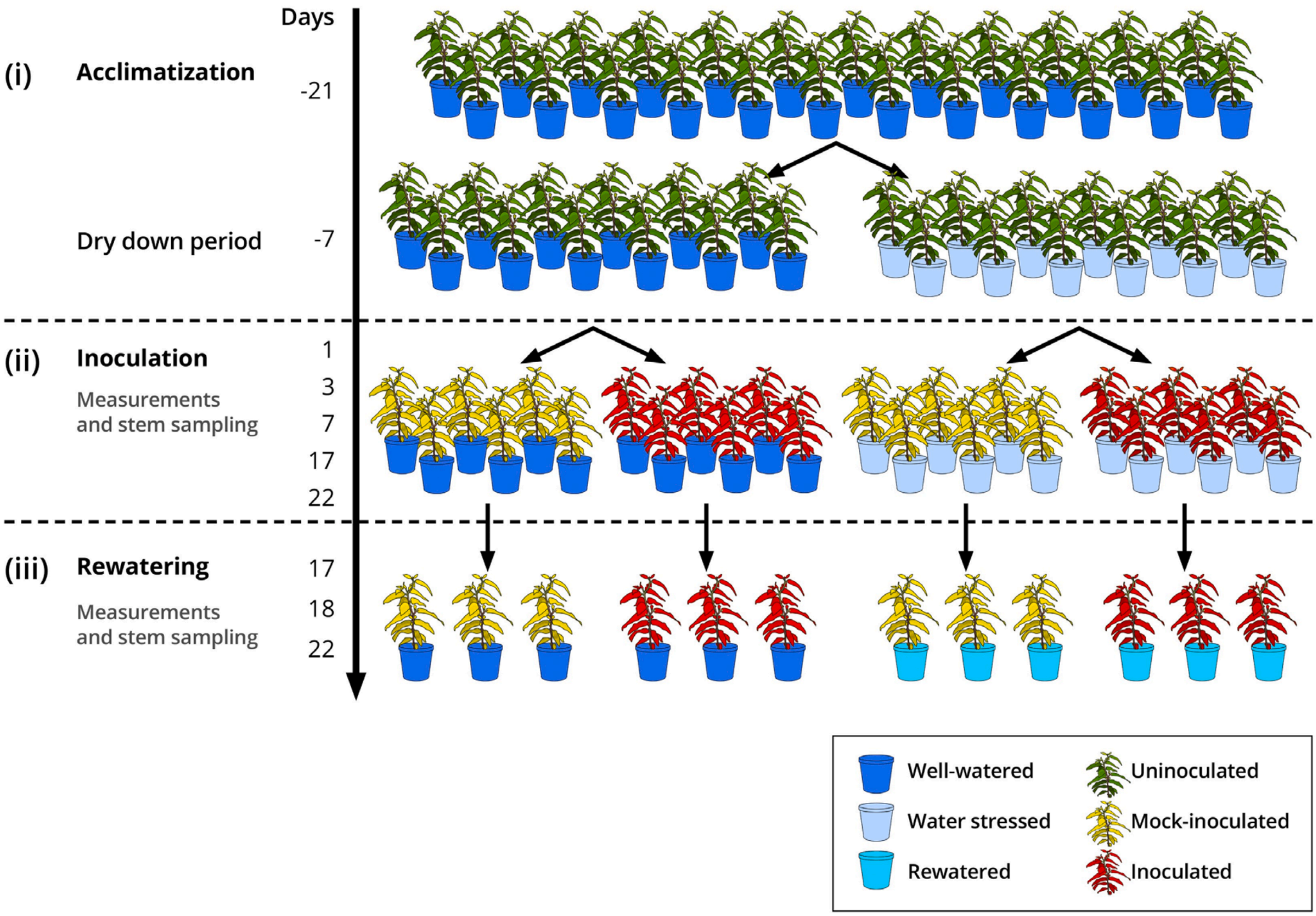

Fig. 1. Treatments and experimental design for the glasshouse experiment on combined drought stress/rewatering and pathogen infection in *Eucalyptus grandis*. The number of trees depicted in the figure are not proportional to the number of trees used for the experiment. A total of 108 plants (36 plants in each phytotron) were transplanted to 10 L pots and acclimatized to the glasshouse conditions. Seven days before inoculation, drought stress was induced by withholding water for 60 pots while the remaining 48 pots were watered every day. In each of the well-watered and water stressed groups, half of the plants were inoculated with *C. austroafricana* while the remaining half was mock inoculated with sterile agar. Twelve plants were rewatered at day 16 from each of the mock inoculated-water stressed and inoculated - water stressed groups. Mock inoculated- well watered and inoculated – well watered plants were used as controls for the different sampling timepoints. Measurements and stem samples were taken from a total of six trees per treatment in each timepoint. The roman numerals indicate the different phases of the experiment i.e acclimatization to the glasshouse conditions and dry down period which respectively started 21 and 7 days before inoculation (i), combined stress treatments (ii), and rewatering treatments (iii). Days 1 and 17 are days of inoculation and rewatering which respectively correspond to 8 and 24 days of withholding water. Days 3, 7, 17, 18, and 22 are days of measurement and stem sampling and respectively correspond to 10-, 14-, 24-, 25-, and 29-days after withholding water. Stem samples, 2 cm in length flanking the (mock) inoculation point, were destructively harvested. In (iii), days 17, 18, and 22 represent 1 day before and 1 and 5 days following rewatering. The colours of pots and trees represent watering and inoculation conditions, respectively.

identified those which were DE in one or more of the rewatering treatments (Methods S1). We also identified transcription factors (TF), whose target genes were significantly overrepresented in each set of unique and shared DEGs identified by Venn intersection and selected TFs, significantly DE in one or more of the rewatering treatments.

For the pathogen transcripts, we selected the top 100 highly expressed genes (top 100 genes) for each treatment and compared the expression patterns with *in vitro* and *in planta* RNA-seq data from previous studies (Mangwanda et al., 2015; 2016). We also computed DE and identified DEGs specifically related to pathogenicity (Methods S1). Finally, we visualized the expression pattern of selected host and pathogen genes using heatmaps.

2.3. *Co-expression network construction and identification of key modules and hub genes*

After checking for a possible batch effect among the different RNA-seq data sets and conducting batch correction (Fig. S2a,b), we constructed two co-expression networks consisting of ‘unstressed’ and ‘stressed’ sets of samples (Fig. S3a; Methods S2) using Pearson correlation coefficient to measure co-expression between genes and Weighted Gene Co-expression Network Analysis (WGCNA) to detect co-expression modules (Langfelder & Horvath, 2008) with at least 50 genes in a module. This was followed by calculation of module eigengenes and merging close modules.

We employed two different methods for the identification of modules of interest from the two networks (Methods S2). For the network of the ‘unstressed’ samples, we conducted module preservation analysis (MPA) where we used the ‘unstressed’ set of samples as a reference. We used composite module preservation statistics $Z_{summary}$ and *medianRank* to identify unpreserved modules (Langfelder et al., 2011). For the network of the ‘stressed’ set, we used the correlation between module eigengenes and experimental conditions (module-trait correlation analysis, MTCA) to identify modules showing strong correlations with the target experimental conditions. Then, we identified hub genes from key modules selected by MPA and MTCA.

3. Results

3.1. Pathogen infection does not cause a further reduction in stomatal conductance under combined stress but delays the recovery of stomatal conductance upon rewatering

We conducted a glasshouse experiment involving combined drought stress and infection by *C. austroafricana* as well as rewatering following these stresses using two-year-old ramets of the *E. grandis* clone TAG5, which is moderately resistant to the pathogen (Fig. 1). To get an insight into the physiological changes under these conditions, we measured stomatal conductance (*gs*) at different timepoints. As the severity of drought stress progressed (part ii, Fig. 1), *gs* decreased at days 17 and 22 for both mock inoculated and *C. austroafricana* inoculated trees (Fig. 2a). This difference in *gs* between WW and WS was significant ($P < 0.05$) for mock-inoculated trees (WWMI *vs* WSMI, Fig. 2a), while in the pathogen-challenged group, the reduction in *gs* between WWIN and WSIN was lower and not statistically significant. This was caused by a reduction in *gs* in the well-watered conditions in response to the presence of the pathogen (WWIN), while, irrespectively to the presence or absence of the pathogen, drought-stressed trees reached similar values of *gs* (Fig. 2a, Table S1). The apparent reduction of *gs* in the WWIN trees is indicative of an effect of the pathogen on the overall plant physiology.

For the rewatering treatments (part iii, Fig. 1), we observed a statistically significant difference ($P < 0.05$) in *gs* between WW and RW trees only in the inoculated plants at 1 day of rewatering (Fig. 2b, Table S1), suggesting that pathogen infection may have delayed the recovery of *gs*. However, the treatments did not show any detectable difference ($P < 0.05$) in *gs* at a later time point, 5 days of rewatering (Fig. 2b), suggesting that trees were ultimately able to resume carbon assimilation under both single and combined stress conditions.

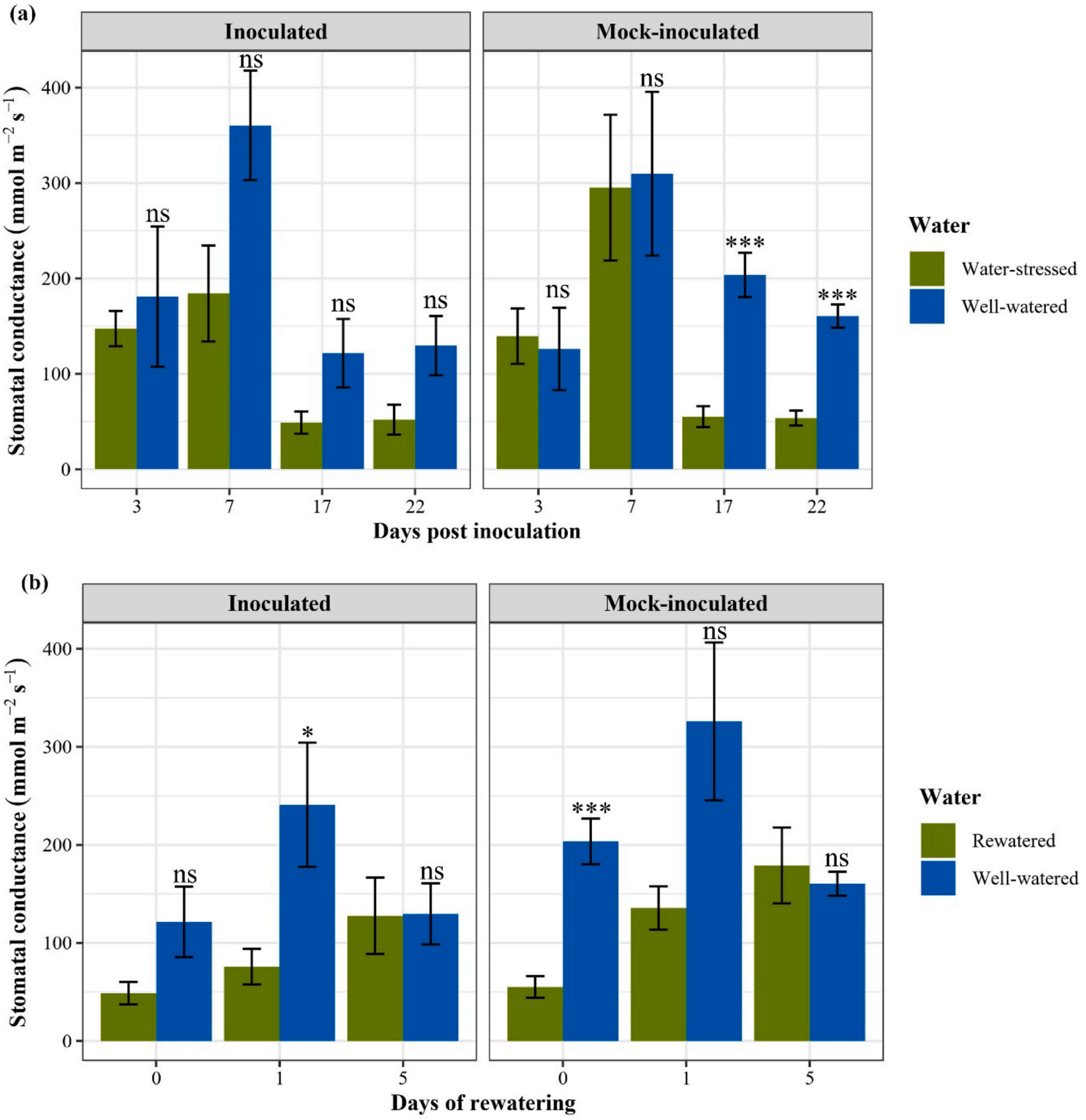

Fig. 2. Stomatal conductance (*gs*) of leaves measured from glasshouse experiments involving drought stress/recovery and pathogen infection in *Eucalyptus grandis*. a. *gs* during drought b. *gs* during recovery. In b, days 0, 1, and 5 respectively correspond to 17-, 18-, and 22-days post inoculation. Pairwise *t*-test, ns, not significant; *, $P < 0.05$; ***, $P < 0.001$.

3.2. Mild drought stress increases stem lesion length while rewatering causes no detectable change during recovery from combined stress

To monitor disease progression in the inoculated trees under different watering conditions, we measured stem lesion length at different timepoints (Fig. 1, Fig. S4a-i). As a result of fungal infection, we observed a significant difference ($P < 0.05$) in lesion length between inoculated and mock-inoculated treatments in both WW and WS plants at all the measurement timepoints (Fig. 3a), with a gradual increase in lesion length from day 3 to day 22 post inoculation. There was a significant water × inoculation interaction on day 3 (Table S1), and the average lesion length in the inoculated trees was significantly higher ($P < 0.05$) under WS than WW conditions (Fig. 3a) indicating that mild drought stress (Fig. S1a,b) may have increased the susceptibility of trees to pathogen challenge. However, the differences in lesion length were not statistically significant ($P < 0.05$) at later timepoints (Fig. 3a) suggesting that more severe drought may have affected the pathogen as well as the plants. This trend at the later timepoints did not change after rewatering as there was no significant difference ($P < 0.05$) between the lesion lengths of the RWIN and WWIN treatments (Fig. 3b) suggesting that rewatering did not impact disease progression at least in the short term.

3.3. Drought-induced changes in host defense related signalling pathways contribute to increased susceptibility to pathogen infection under combined stress conditions

As 3 dpi has been established as a key timepoint to explore the transcriptomic responses of *E. grandis* to *C. austroafricana* infection (Mangwanda et al., 2015) and as we observed significantly longer stem lesion under combined stress (Fig. 3a), we used stem samples from day 3 (Fig. 1) for RNA-seq analysis. To compare the transcriptomic changes of the moderately resistant genotype, TAG5, under combined stress with that of unstressed and single stressed samples of TAG5 and ZG14, we included RNA-seq data from previous studies (Mangwanda et al., 2015; Teshome et al., 2020) into our analyses (Methods S1). To compare the changes in co-expression patterns due to individual and combined stresses and identify key signalling pathways and genes related to the response of trees to these stresses, we constructed two co-expression networks by dividing the RNA-seq data into an 'unstressed' set, including either unwounded or mock-inoculated well-watered samples and a 'stressed' set, including samples exposed to *C. austroafricana* infection, drought stress, or a combination of both stresses (Fig. S3a; Methods S2).

To investigate changes in network properties between the 'unstressed' and 'stressed' sets, we performed a module preservation analysis (MPA, Fig. S3b) and identified modules of the 'unstressed'

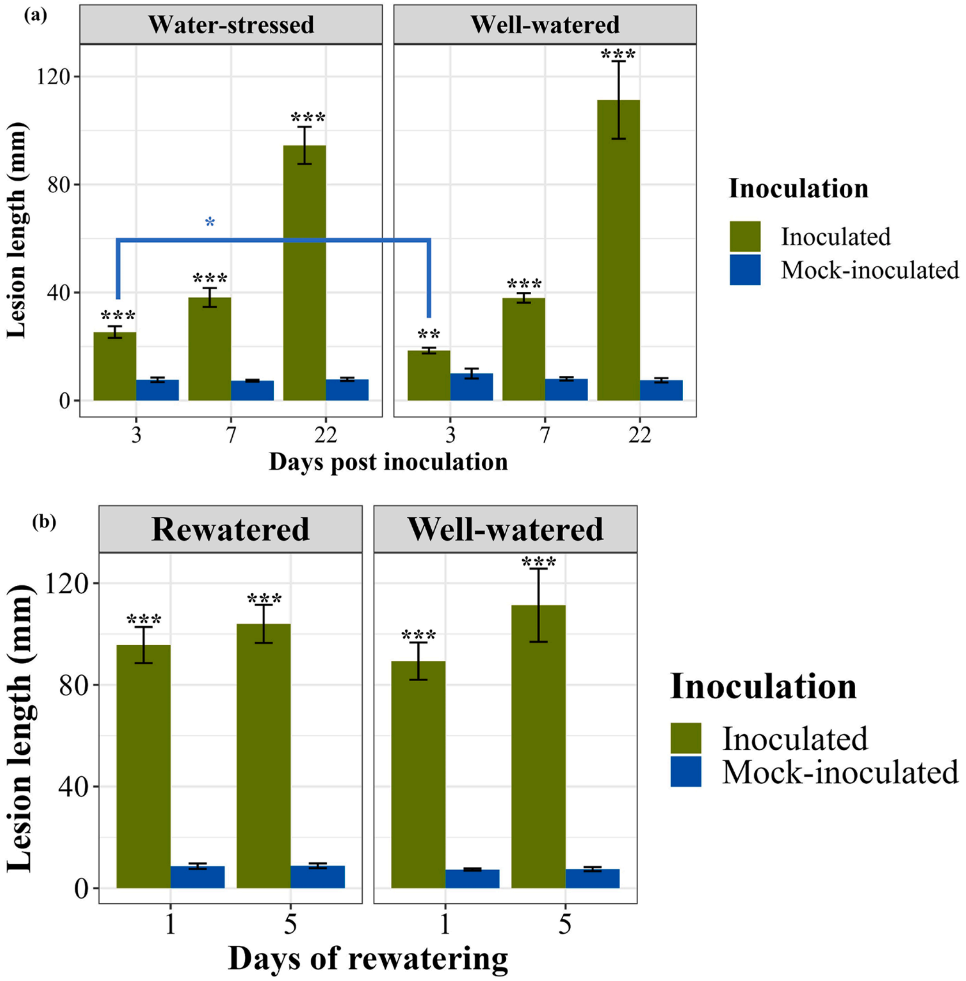

Fig. 3. Stem lesion development in 2-year-old *Eucalyptus grandis* trees under drought stress/recovery-pathogen infection glasshouse experiment. a. lesion length measurements during drought. For the water-stressed group, days 3, 7, and 22 correspond to 10-, 14-, and 29-days of withholding water. b. lesion length measurements during recovery. For the rewatered group, plants were rewatered at 17 days post inoculation which corresponds to 24 days of withholding water. In b, days 1 and 5 respectively correspond to 18- and 22-days post inoculation. The lesion length data are represented as mean + SE. Pairwise *t*-test, *, $P < 0.05$; **, $P < 0.01$; ***, $P < 0.001$.

reference network with either minimal (preserved, 19 modules) or significant (unpreserved, 20 modules) changes in network properties when tested against the ‘stressed’ samples. As the unpreserved modules indicate network perturbations due to stress, we conducted functional enrichment analyses in these modules to get an overview of the molecular changes underlying responses to the stresses (Fig. 4a; Table S2). This included the *darkgreen* module (Fig. S3b), enriched with several GO terms related to known pathogen responses in *E. grandis* such as SA signalling pathways (Fig. 4a; Table S2; Mangwanda et al., 2015), and the *darkslateblue* module (Fig. S3b), enriched with GO terms associated with responses to abiotic stresses including responses to heat and reactive oxygen species (Fig. 4a; Table S2; Teshome et al., 2023). In the highly unpreserved *floralwhite* module (Fig. S3b), the GO term secondary cell wall biogenesis was the only term enriched (Fig. 4a; Table S2). Furthermore, TF enrichment analysis in these modules identified potential regulators of single and combined biotic and abiotic stress responses including potential members of the WRKY, MYB, and HSF families (Table S3). These results highlight that module preservation analysis is able to identify potential key molecular actors and regulators that play a role in the interaction between drought stress and pathogen infection. Thus, these three modules were selected as key unpreserved modules for further analysis.

To investigate the molecular processes and key genes specifically related to tree responses to combined stress, we correlated the experimental conditions with the average profile of each module of the co-expression network built for the ‘stressed’ set. As disease progression was enhanced under mild drought stress (Fig. 3a), we explored modules correlated with the combined stress treatment and the susceptible genotype under pathogen infection (WSIN and ZG14IN, Fig. S3c) to identify possible mechanisms of drought-induced susceptibility to the pathogen. We found three and seven modules significantly correlated with the combined stress treatment and the susceptible genotype ($r \geq 0.53$, $P < 0.05$), respectively (Fig. S3c). Notably, GO terms related to metabolism and abiotic stress responses (Fig. 4b, Table S4) as well as several TFs involved in the ABA, ET, and brassinosteroid (BR) signalling pathways (Table S3) were significantly enriched (Benjamini–Hochberg adjusted *P*-value (BH *P*-value) < 0.05) in the *saddlebrown* module. In the *darkolivegreen* module, GO terms related response to pathogen such as response to chitin, respiratory burst involved in defense response, and ET mediated signalling pathway (Fig. 4b, Table S4) as well as TFs such as the putative orthologs of *MYB61, ANAC075, ERF48*, and *ARF16* (Table S3), known to be involved in secondary cell wall formation (Hussey et al., 2013; Zhong et al., 2021) and hormonal cross-talks related to growth and abiotic stress response (Chen et al., 2010; Mei et al., 2023), were significantly enriched (BH *P*-value < 0.05). Furthermore, visualization of the expression of genes in the highly correlated modules (Fig. S5a-j) as well as unpreserved modules (Fig. S5k-m) using heatmaps revealed that the combined stress treatment (INWS) clustered closer to the susceptible (ZG14) than the moderately resistant (TAG5) genotype in some of the modules such as the *darkolivegreen* module (Fig. S5e). These results suggest that drought stress may have triggered transcriptomic changes in the moderately resistant genotype under combined stress, similar to that of the susceptible one under the single stress of pathogen infection, consistent with the observed increase in disease progression under combined stress (Fig. 3a).

We identified a total of 393 hub genes from the 13 key modules that were found to be associated with the combination of stresses (selected using MPA and MTCA; Methods S2; Table S5). This included the putative orthologs of *NPR1*, a key regulator of SA-mediated defense and hormonal crosstalk (Backer et al., 2019), *BIP1*, a member of the HSP70 family that are induced by abiotic stresses such as heat stress (Koizumi, 1996), *ACO4*, a gene involved in ET biosynthesis (Gómez-Lim et al., 1993), and several uncharacterized genes selected for modules unpreserved in response to stress (Table S5). The putative orthologs of *NPR1* and *ACO4* were downregulated only under the combined stress treatment, while that of *BIP1* was upregulated (Fig. 5a, Table S5). As these genes underlie network perturbation due to stress, they could be related to pathogen infection, drought stress, and/or their combination, although it is not possible to establish whether these genes specifically mediate the response during the combination of stresses. To detect genes possibly involved in governing combined stress response, we identified hub genes from the modules correlated with the combined stress treatment including the putative orthologs of *AAE18*, involved in the activation of auxin precursors (Wiszniewski et al., 2009) and *VDAC1*, which encodes an anion channel related to pathogen-induced ROS production (Tateda et al., 2011). Both genes were upregulated only under combined stress (Fig. 5b, Table S5). Similarly, we identified hub genes from the modules correlated with the susceptible genotype including the putative orthologs of *HSPRO2*, which regulates basal resistance (Murray et al., 2007), *BGAL8*, a gene in the β-galactosidase family that includes genes such as *OsBGAL9*, which confers disease resistance and heat tolerance (Hoang et al., 2023), and several uncharacterized genes (Table S5). These genes were respectively downregulated and upregulated only

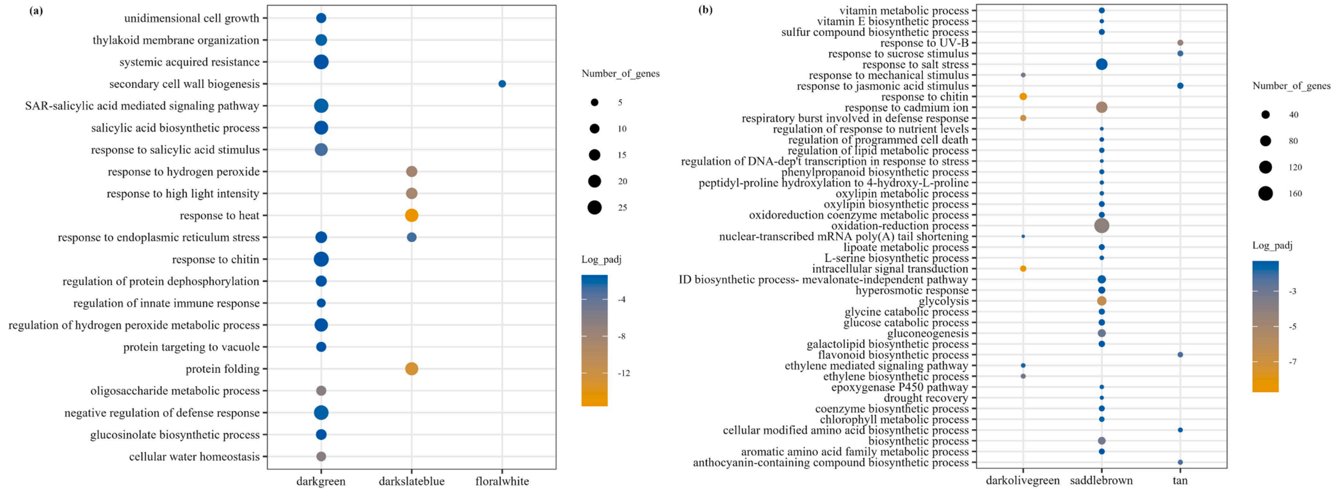

Fig. 4. Gene ontology biological process (GO) enrichment for key co-expression modules selected using module preservation (MP) and module trait correlation (MTC) analyses. a. modules selected using MP b. modules selected using MTC. The R package GO-seq was used for GO enrichment analysis. The significantly overrepresented GO terms (Benjamini-Hochberg adjusted *P*-value < 0.05) were visualized in dot plots generated using R. The color and size of dots respectively represent the $\log_{10}$ adjusted *P*-value and number of genes.

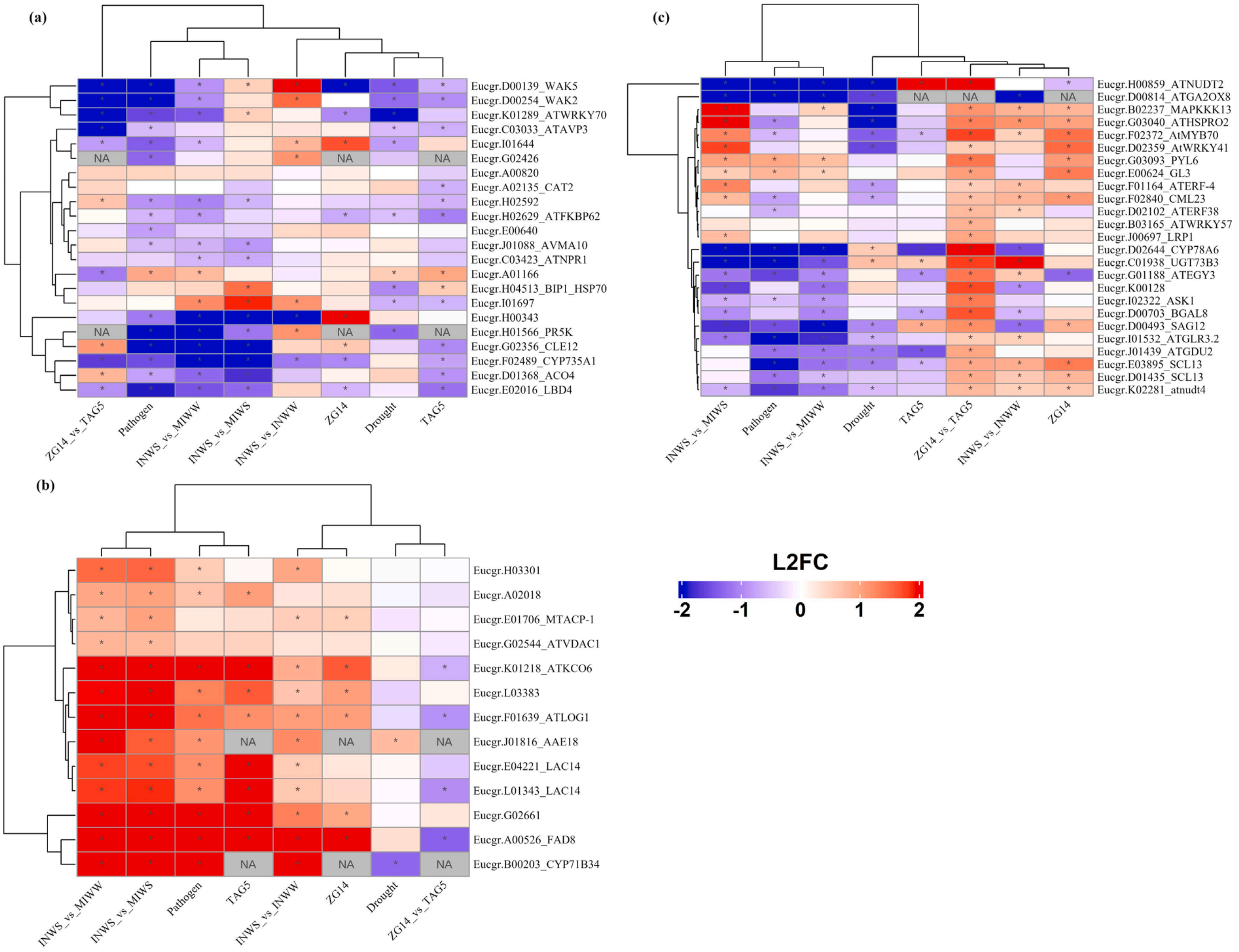

Fig. 5. Selected hub genes identified from key co-expression modules. a. Hub genes selected from key unpreserved modules b. Hub genes selected from modules correlated with the combined stress treatment c. Hub genes selected from modules correlated with the susceptible genotype. The details of all hub genes identified from all the key modules is given in Table S5. The $\log_2$ foldchange (L2FC) between different comparisons was used to plot the heatmap using the R package ComplexHeatmap. * Indicates a L2FC $> |0.5|$. MIWW = Mock-inoculated-well-watered, MIWS = Mock-inoculated-water-stressed, INWW = Inoculated-well-watered, INWS = Inoculated-water-stressed, TAG5 and ZG14 refer to comparisons between the respective inoculated and mock-inoculated treatments using the data from Mangwanda et al., (2015), drought and pathogen respectively refer to comparisons of MIWS and INWW with MIWW based on the data from the present experiment.

under combined stress (Fig. 5b, Table S5), suggesting increased host susceptibility due to drought stress.

Among the 393 hub genes identified in the modules of interest, several genes showed expression pattern in the moderately resistant genotype under combined stress similar to that of the susceptible one under the single stress of pathogen infection (Fig. 5a-c, Table S5). This included the potential orthologs of genes such as *SCL13*, a putative positive regulator of GA accumulation (Zhang et al., 2011), *AtGA2OX8*, a gene which inactivates GA (Schomburg et al., 2003), *AtERF4*, a negative regulator of JA/ET-induced defense genes (McGrath et al., 2005), *MAPKKK13*, a gene that induces the ET biosynthesis gene *ACS8* (Li et al., 2018; Sözen et al., 2020), and several uncharacterized genes. The putative orthologs of *SCL13* were downregulated only under the single stress of pathogen infection, while those of *AtERF4* and *MAPKKK13* were induced only under combined stress (Fig. 5c, Table S5). While the putative ortholog of *AtGA2OX8* was downregulated under both the single stress of pathogen infection and combined stress, the reduction in expression was higher under combined stress (Fig. 5c, Table S5). Overall, the identified hub genes may involve key drivers of tree response to combined stress and provide molecular evidence to the enhanced disease progression observed in the moderately resistant *E. grandis* genotype. In this regard, these genes with similar expression pattern to the susceptible genotype could more likely be related to drought-induced susceptibility to the pathogen under combined stress.

3.4. Rewatering following exposure to combined stress triggers distinct transcriptomic changes indicating a trade-off between stress response and growth in the plants

To understand the transcriptomic changes during rewatering following combined stress, we conducted RNA-seq analysis using stem samples from day 18, which corresponds to 1 day of rewatering (Fig. 1). We identified genes, DE under one or more of the single stress of pathogen infection (PI), recovery from the single stress of drought (RD), and recovery from the combined stresses of drought and pathogen infection (RDPI) using Venn intersection analysis (Fig. 6a) and conducted GO and TF enrichment analyses (Fig. 6b,c) followed by investigation of selected specific genes (Fig. 7a-f), which together revealed distinct transcriptomic changes during RDPI.

Several GO terms related to the biosynthesis and signalling pathways of JA and ET were enriched in the upregulated DEGs shared between RDPI and PI (Fig. 6b; Table S6). Some genes related to JA biosynthesis

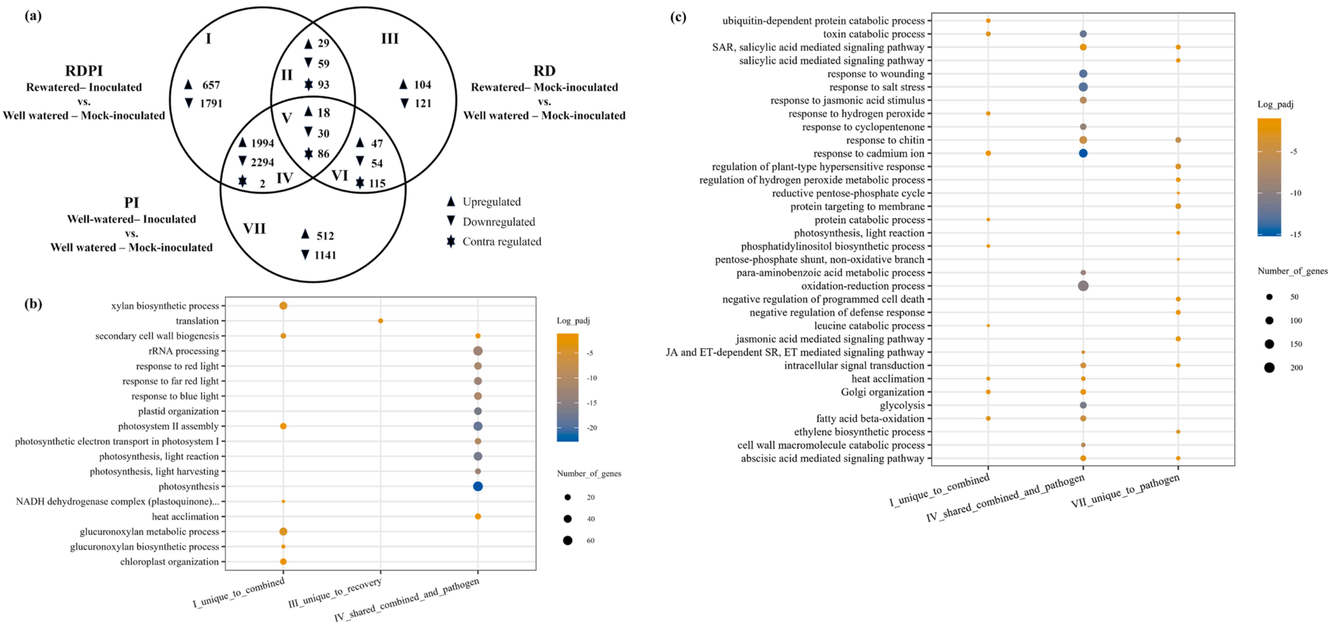

Fig. 6. Transcriptomic changes during recovery from combined drought stress and pathogen infection in *Eucalyptus grandis*. a. Venn-intersection of differentially expressed genes (DEG) for recovery from drought stress at 1 day following rewatering (RD), pathogen infection at 18 days post inoculation (PI), and recovery from combined drought stress and pathogen infection at 1 day following rewatering (RDPI). Stem samples collected from the rewatering experiment indicated in part iii, Fig. 1, were used for RNA-seq analysis for these treatments b. GO enrichment for downregulated DEGs unique to and shared between PI, RD, and RDPI c. GO enrichment for upregulated DEGs unique to and shared between PI, RD, and RDPI. For the set of DEGs shared between RDPI and PI, only the top 10 highly enriched GO terms were included in the figures. All the enriched GO terms (Adjusted *P*-value < 0.1) are given in Table S3. The roman numerals indicate the different Venn intersections representing shared and unique sets of DEGs in a and the respective GO terms enriched in these sets of DEGs in b and c.

including *EgrLOX2* were uniquely upregulated under RDPI (Fig. 7a; Table S7). Additionally, a potential ortholog of *WRKY22*, which induces *MYC2*, a negative regulator of the JA/ET-induced defense genes (Kloth et al., 2016), was one of the enriched TFs, and both of these genes were uniquely downregulated under RDPI (Fig. 7a,d). Some JA/ET-induced defense genes including *EgrPR4*, a marker for JA signalling in *E. grandis* (Naidoo et al., 2013), were upregulated under both PI and RDPI. *EgrPR3* and two other genes encoding potential homologs of *PR3* were upregulated under PI and RDPI but downregulated under RD. On the other hand, the putative orthologs of *AtICS2*, a gene involved in SA biosynthesis, as well as *AtMES10* and *AtSAGT1*, genes involved in the formation of inactive conjugates of SA, were respectively down- and upregulated only under RDPI (Fig. 7b). Overall, our transcriptomic data suggests that the JA/ET signalling pathways could be key players of recovery from drought under combined stress conditions.

The GO terms such as cellular water homeostasis, water transport, and cellular cation homeostasis were enriched in the downregulated DEGs shared between PI and RDPI (Fig. 6c; Table S6), while the GO terms response to ABA and water deprivation, proline transport, and carbohydrate metabolic process were enriched in the upregulated DEGs indicating the plants' response to dehydration related to impairment of water transport possibly caused by the pathogen (Fig. 6b; Table S6). The ABA induced gene *EgrNAC123*, one of the enriched TFs (Table S8), was upregulated under both PI and RDPI but showed a further increase in expression in the later (Fig. 7c). The putative ortholog of *ABF2*, a TF which regulates ABA-induced genes (Yoshida et al., 2010), was another enriched TF (Table S8) uniquely upregulated under PI (Fig. 7d) suggesting that the ABA-dependent pathway could be important under PI. On the other hand, *EgrDREB2.5*, a marker of the ABA-independent pathway in *E. grandis* (Nguyen et al., 2017) was uniquely upregulated under RDPI (Fig. 7c) suggesting that this pathway could be more important during RDPI. Furthermore, several genes potentially encoding HSPs, were uniquely upregulated under RDPI (Fig. 7c, Table S7) indicating that more stress responsive genes were induced during RDPI. Overall, these results indicate the importance and differential regulation of abiotic stress responsive genes during RDPI compared to PI.

The GO terms starch biosynthetic process, response to auxin stimulus, and several terms associated with photosynthesis were overrepresented in the downregulated DEGs shared between RDPI and PI (Fig. 6c, Table S6). Additionally, the GO terms chloroplast organization, photosystem II assembly, and secondary cell wall biosynthesis were enriched in the downregulated DEGs unique to RDPI (Fig. 6c). The potential orthologs of genes involved in sucrose degradation, stachyose and starch biosynthesis including *FLN1, AtGolS2, AtSTS*, and *APL2*, were uniquely downregulated during RDPI, while genes involved in trehalose biosynthesis such as *ATTPS1* and *ATTPS2* were uniquely upregulated (Fig. 7e; Table S7) suggesting a reduction in carbohydrate storage during RDPI. In contrast, genes involved in starch and stachyose biosynthesis such as *SIP1* and *ATSS3* were uniquely upregulated during RD. Furthermore, several genes related to cell wall formation were uniquely downregulated under RDPI (Fig. 7f; Table S7). Notably, *EgrMYB46*, an ortholog of *AtMYB46* (Brown et al., 2019), a key transcriptional regulator of secondary cell wall formation (Hussey et al., 2013; Ko et al., 2014), was one of the enriched TFs uniquely downregulated under RDPI (Fig. 7d; Table S8). Together, our transcriptomic data suggests that secondary cell wall formation and carbohydrate storage could have been compromised under RDPI possibly due to reallocation of carbon towards stress response-related functions.

3.5. *Transcriptomic changes in the pathogen suggest alterations in fungal metabolism and interaction with the host during drought stress and subsequent rewatering*

To get an insight into how the pathogen thrives in its tree host under drought stress and subsequent rewatering, we investigated the changes in the *in planta* fungal transcriptome using RNA-seq data on days 3 and 18 of the moderately resistant genotype, TAG5, inoculated with *C. austroafricana* (Fig. 1; Methods S1). We compared these changes with *in planta* fungal transcriptome in the susceptible genotype, ZG14, and *in vitro* on minimal media using RNA-seq data from a previous study

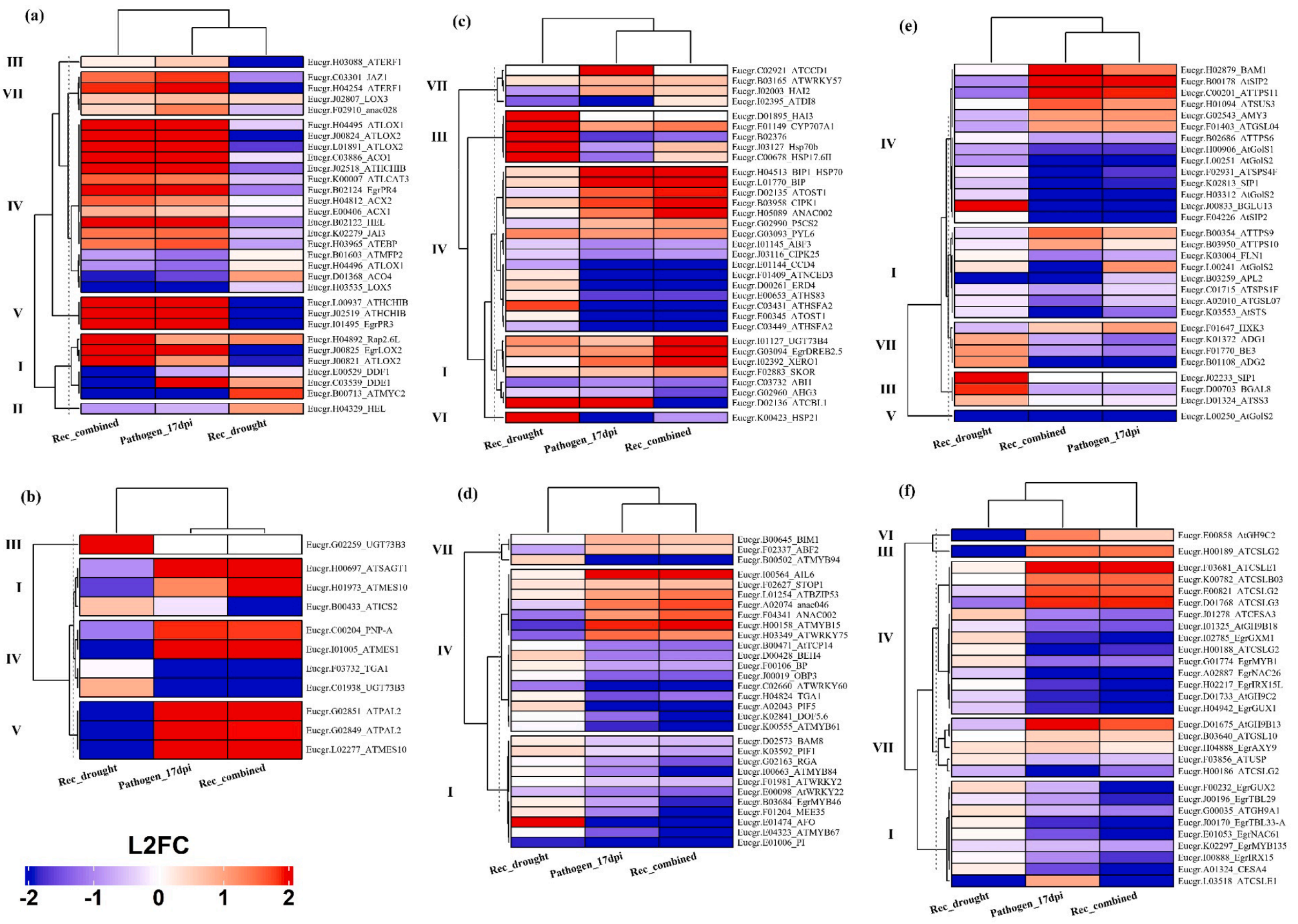

Fig. 7. Expression pattern of selected key genes potentially involved in different molecular process and signalling pathways during recovery from single and combined stress conditions in *Eucalyptus grandis*. a. jasmonic acid/ethylene b. salicylic acid c. drought response d. transcription factors e. non-structural carbohydrate metabolism f. cell wall. The $\log_2$ foldchange (L2FC) between different comparisons was used to plot the heatmap using the R package ComplexHeatmap. The Roman numerals indicate genes differentially expressed under a specific condition (unique DEGs) or under two or more of the conditions (shared DEGs) representing the different Venn intersections shown in Fig. 6a, *i.e.* I = unique to recovery from combined stress, II = shared between recovery from combined stress and the single stress of drought, III = unique to recovery from the single stress of drought, IV = shared between recovery from combined stress and the single stress of pathogen infection, V = shared among the single stress of pathogen infection, recovery from combined stress, and recovery from the single stress of drought, VI = shared between the single stress of pathogen infection and recovery from the single stress of drought, VII = unique to the single stress of pathogen infection. The full list of selected genes with detailed descriptions and basis for selection of each gene is given in Tables S2 and S4.

(Mangwanda et al., 2016). The top 100 genes in the WW treatment on day 3 showed a reduction in expression under WS conditions and clustered with that of infected ZG14, supporting a susceptible interaction under drought stress (Fig. 8a). The top 100 genes in the WS treatment on day 3 showed both an increase and decrease in expression compared to the WW condition (Fig. 8b). Upon rewatering, the expression of the top 100 genes mostly increased under the RW treatment compared to the WW control (Fig. 8c,d). Furthermore, GO enrichment analysis on these sets of genes suggested that there was also a change in the function of the highly expressed genes under drought stress and rewatering (Fig. 8e).

To identify key fungal genes underlying the changes in *C. austroafricana* under drought stress and rewatering, we selected genes with a significant L2FC (adjusted *P* value < 0.05) as DEGs for WS and RW in comparison to the respective WW controls (Table S9). We classified the fungal DEGs with a percent identity of at least 60 % into different pathogenicity related categories curated by the pathogen host interactions database (PHI-base) (Urban et al., 2022) (Fig. 9a, Table S9). In the lethal category, two potential orthologs of the *Fusarium graminearum* TFs *GzOB014* and *GzOB009* (Son et al., 2011) were downregulated during drought stress. In the loss of pathogenicity category, genes related to fungal metabolism and transport such as the putative orthologs of *PTH3*, a histidine biosynthesis gene (Sweigard et al., 1998), *GNA1*, a gene involved in chitin biosynthesis (Lockhart et al., 2020), *PTH2*, a lipid transporter (Bhambra et al., 2006), and *Neo1*-like Calcium-transporting ATPase 3 (Nguyen et al., 2008) were upregulated while genes involved in fungal growth such as *MST50p* and *Vph1* (Kramer et al., 2009; Sarmiento-Villamil et al., 2018) were downregulated during drought. In the reduced virulence category, genes involved in fungal metabolism and stress response such as the putative orthologs of *AOX1* (Segers et al., 2001) and *FpHsp104* (Xia et al., 2021) were upregulated while those related to growth and reproduction such as *MoIlv1* (Du et al., 2014), *MoPyr5* (Qi et al., 2016), and *CPKK1* (Moretti et al., 2014) were downregulated. These results suggest that the pathogen may have maintained its metabolism under drought stress, while its *in planta* growth could have been compromised.

To investigate the impact of drought stress and rewatering on the pathogenicity of *C. austroafricana*, specifically with respect to cell wall degrading enzymes (CWDE), we conducted a BLASTp search on the carbohydrate-active enzyme annotation database, dbCAN3 (Yin et al., 2012) (Fig. 9b, Table S9). Genes potentially encoding glycosyl transferase (GT) family proteins, related to strengthening fungal cell wall and other adaptive responses (Klutts et al., 2006; Grille et al., 2010) as well

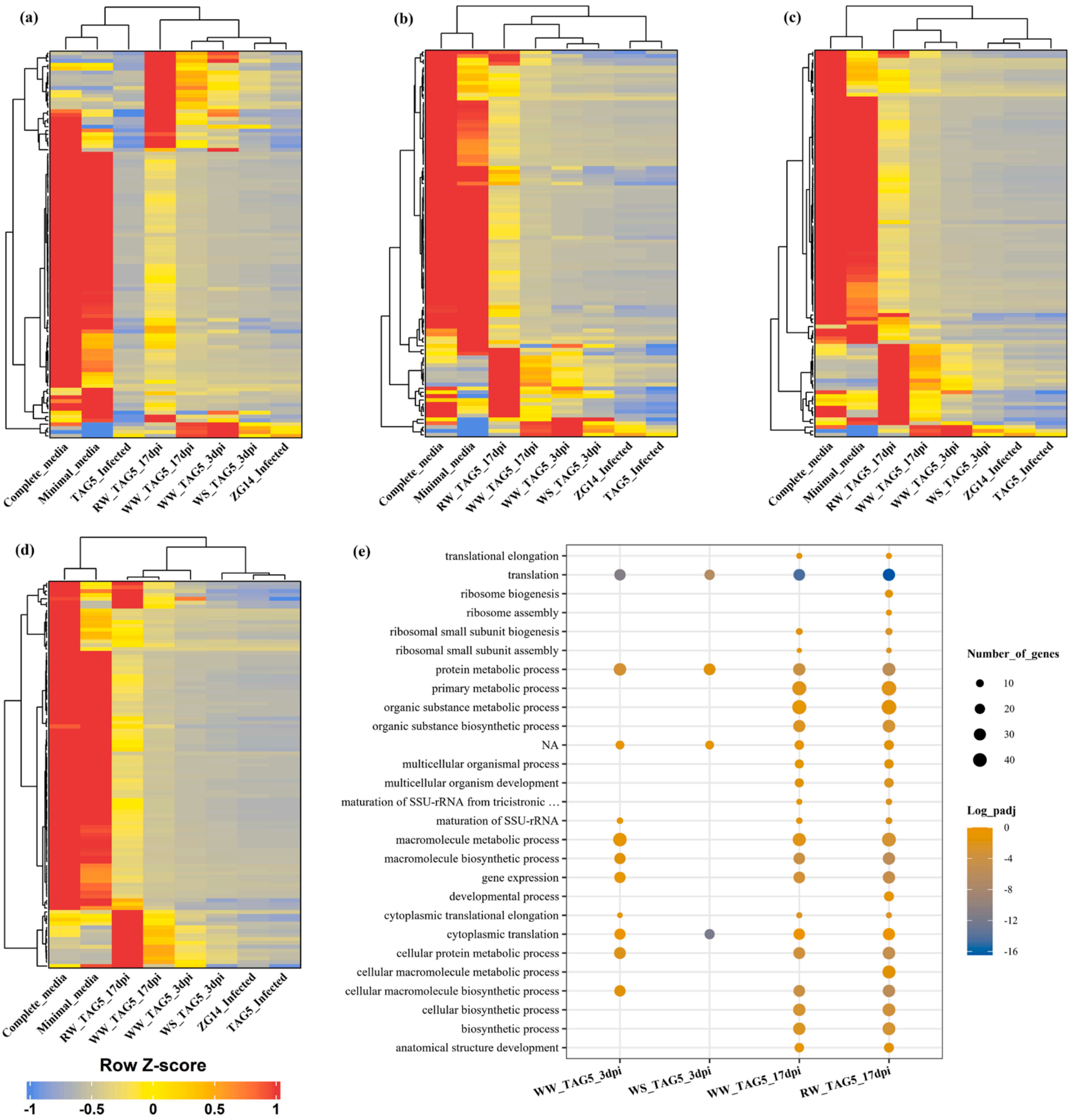

Fig. 8. Top 100 highly expressed genes of Chrysoporthe austroafricana under drought stress and subsequent rewatering in *Eucalyptus grandis*. a. well-watered (WW) treatment on day 3 b. water stressed (WS) treatment on day 3 c. WW treatment on day 18 d. rewatered (RW) treatment on day 18. The row Z-score representing normalized relative transcript abundance was used to plot the heatmap using the R package ComplexHeatmap. ZG14 and TAG5 are *E. grandis* genotypes, susceptible and moderately resistant to *C. austroafricana*, respectively. e. enriched gene ontology biological process (GO) terms in each set of highly expressed genes. The R package GO-seq was used for GO enrichment analysis. The significantly overrepresented GO terms (Benjamini-Hochberg adjusted *P*-value < 0.05) were visualized in a dot plot generated using R. The color and size of dots respectively represent the $\log_{10}$ adjusted *P*-value and number of genes.

as those potentially encoding enzymes such as glycoside hydrolases (GH) that degrade pectin and cellulose were upregulated during drought. However, several other genes potentially encoding GH related to cellulose, hemicellulose, and pectin degradation (Rafiei et al., 2021) were downregulated. These results suggest a prioritization of survival in the drought-stressed host environment by strengthening the fungal cell wall and reducing the expression of several CWDEs.

To gain further information on the overall performance of the pathogen under drought stress and rewatering, we identified several DEGs with known functions in other pathogens but have not been necessarily related to pathogenicity (Fig. 9c; Table S9). This included three upregulated DEGs potentially encoding major facilitator superfamily (MFS) transporters, necessary for protection against plant defense such as ROS (Chen et al., 2017), SA (Chen et al., 2021), and glucosinolates (Vela-Corcía et al., 2019). Genes potentially encoding short-chain alcohol dehydrogenase and carbohydrate and acetate

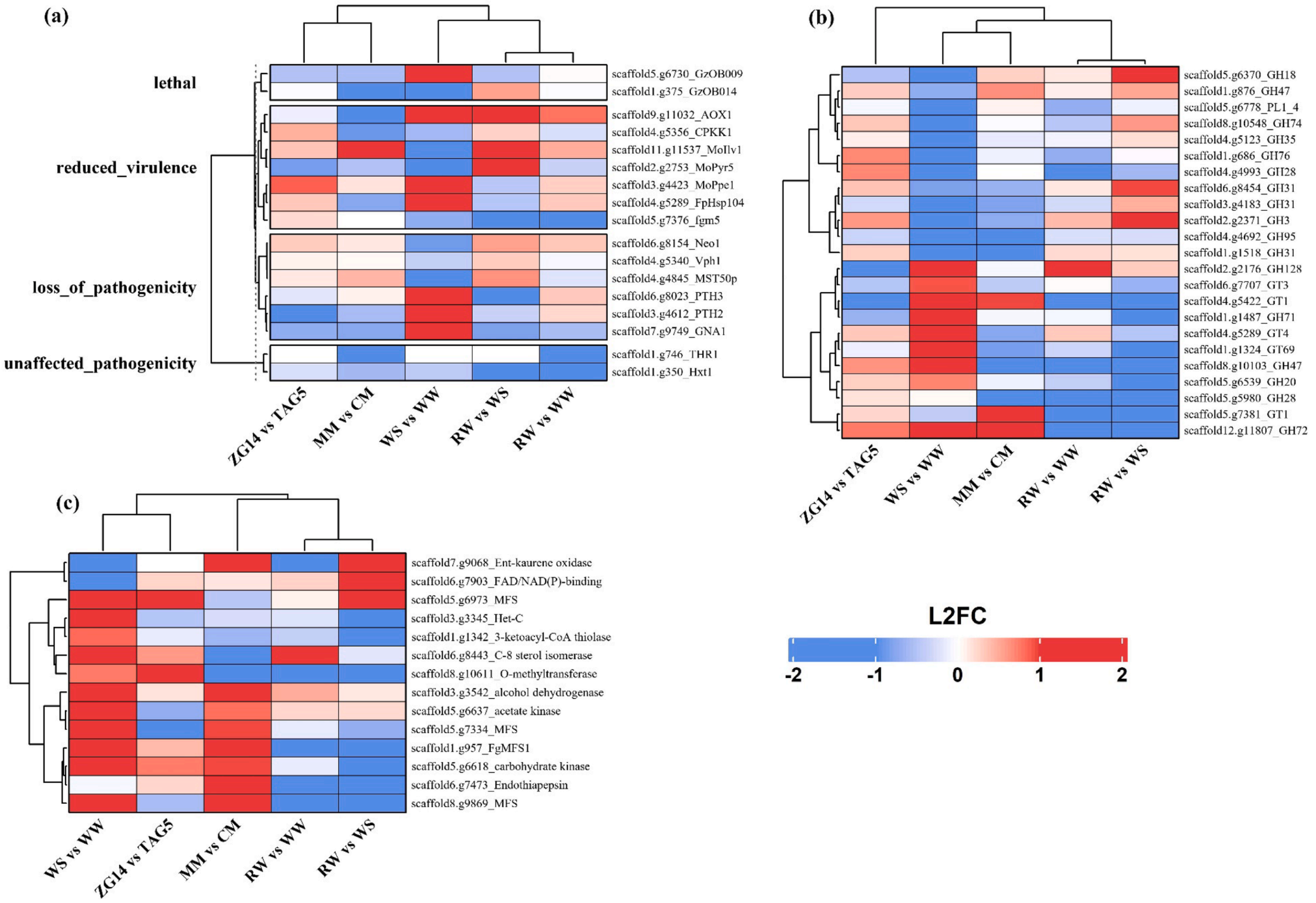

Fig. 9. Selected differentially expressed genes (DEGs) of Chrysoporthe austroafricana under drought stress and subsequent rewatering in *Eucalyptus grandis*. a. DEGs with a BLASTp hit on the pathogen host interactions database (PHI-base) b. DEGs with a BLASTp hit on the carbohydrate-active enzyme annotation database (dbCAN3) c. other DEGs with known function in other pathogens. The $\log_2$ foldchange (L2FC) between different comparisons was used to plot the heatmap using the R package ComplexHeatmap. The full list of DEGs with detailed descriptions for each gene is given in Table S9. ZG14 and TAG5 are *E. grandis* genotypes, susceptible and moderately resistant to *C. austroafricana*, respectively. WW = well-watered, WS = water-stressed, RW = rewatered, MM = minimal media, CM = complete media.

kinases, related to fungal metabolism and are necessary for the survival of the pathogen were also upregulated. Genes potentially encoding FAD/NAD(P)-binding proteins and potential orthologs of the *Valsa mali* ent-kaurene oxidase were downregulated during drought. These results suggest that the pathogen may have altered its interaction with its newly susceptible host and prioritized survival in the drought-stressed host.

We identified fewer genes with a significant L2FC (adjusted *P* value < 0.05) during rewatering compared to those during drought stress (Table S9). These included downregulated genes in the unaffected pathogenicity PHI-base category including the potential orthologs of *Hxt1* and *TRH1* (Fig. 9a), related to fungal growth (Liang et al., 2018; Yuan et al., 2021). The putative orthologs of *GH-28, -72,* and *GT1* were also downregulated during rewatering (Fig. 9b). Other genes including the potential orthologs of the *Coniella lustricola* MFS transporter, the *Colletotrichum truncatum* O-methyltransferase, and the *C. parasitica* endothiapepsin were downregulated (Fig. 9c). These results indicate a reversal of some of the drought-induced changes in the pathogen and downregulation of some fungal metabolic pathways upon rewatering following drought stress.

4. Discussion and conclusion

In this study, we found that combined stress conditions enhanced disease progression at early timepoints during drought (Fig. 3a), suggesting that mild drought stress could have increased susceptibility to pathogen in the moderately resistant *E. grandis* genotype, TAG5, while pathogen infection delayed the recovery of *gs* during rewatering (Fig. 2b), suggesting a possible impairment or blockage of the vascular system limiting water movement (da Silva et al., 2018; Aguirre et al., 2024) and/or phytohormones such as ABA, JA, and ET possibly inhibiting stomatal opening (Förster et al., 2019; Yao et al., 2021). Although there was no detectable difference in *gs* at the early timepoints (Fig. 2a) despite the decrease in soil moisture content (Fig. S1a,b), this could be related to fast root growth under mild drought stress, which increases the absorption of available water and possibly delays responses such as stomatal closure, as has been previously shown in *Eucalyptus* (Li & Wang, 2003; Susiluoto & Berninger, 2007; Amrutha *et al.*, 2019). While evaporation from the soil could contribute to the reduction in soil moisture content, this would have been minimal, particularly after a short phase of soil surface evaporation that forms a dry surface layer leading to a reduction of evaporation from the deeper soil (Han & Zhou, 2013). *Chrysoporthe austroafricana* has been suggested to be either a necrotroph (Wingfield, 1989; Gryzenhout et al., 2004) or hemibiotroph (Zwart et al., 2017). Thus, the observed increase in disease progression is consistent with the model in Oliva et al. (2014) which hypothesized that the combinatorial effect of drought stress and necrotrophic/hemibiotrophic pathogen attacks may be more rather than less damaging to plants. However, the enhancement of disease progression diminished at later timepoints (Fig. 3a), and this pattern did not change up to five days following rewatering (Fig. 3b) suggesting that more severe drought (Fig. S1a,b) may also have affected the pathogen (Zarattini et al., 2021) as has been shown for *C. austroafricana* using *in vitro* experiments where media with lower water potential reduced fungal growth (Swart et al., 1992).

Investigation of the host transcriptome using co-expression network analysis supported increased host susceptibility to the pathogen under drought stress. We found that GO terms related to phytohormone signalling pathways including SA and JA/ET, involved in defense against *C. austroafricana* (Mangwanda et al., 2015), were overrepresented in the identified co-expression modules (Fig. 4a,b). We also identified key genes related to defense signalling pathways with altered expression under combined stress (Fig. 5a-c). Notably, we found an increase in the relative expression of the putative orthologs of *SCL13* and reduction in that of *AtGA2OX8* under combined stress which could contribute to an increased GA concentration, and hence, support increased susceptibility to the pathogen (Mangwanda et al., 2015). The increased *SCL13* expression and possible increase in GA concentration could facilitate the degradation of DELLA proteins (Zhang et al., 2011; Lan et al., 2014). As DELLA proteins also repress SA accumulation (Navarro et al., 2008; Lan et al., 2014), these changes will at least abolish decreases in GA and SA levels at 3 dpi which have been shown to lead to moderate resistance to the pathogen (Mangwanda et al., 2015). Furthermore, we found an increase in the relative expression of *MAPKKK13*, a gene that promotes ET biosynthesis (Li et al., 2018; Sözen et al., 2020), and *AtERF4*, a gene that negatively regulates JA/ET-induced defense genes (McGrath et al., 2005). Previously, it has been shown that differential suppression of *ERF2*, which positively regulates JA/ET-induced defense genes (McGrath et al., 2005), contributes to the susceptibility to *C. austroafricana* of ZG14 (Mangwanda et al., 2015). Overall, these changes in the defense related signalling pathways support increased host susceptibility to the pathogen observed under drought stress.

Changes in the pathogen transcriptome under drought stress suggested that the pathogen may have altered its interaction with the host and prioritized maintaining metabolism and strengthening fungal cell wall while downregulating several genes potentially encoding CWDEs to survive in the drought-stressed host. Genes potentially encoding GT and GH were upregulated under drought stress (Fig. 9b). These proteins are involved in strengthening the fungal cell wall (Free, 2013). However, several genes potentially encoding GHs were also downregulated during drought as has been observed when *C. austroafricana* was grown on minimal media (Mangwanda et al., 2016). This suggests that the increased disease progression under drought stress may not be due to increased pathogenicity, at least in relation to CWDEs, but due to increased host susceptibility. However, downregulation of some CWDEs may not necessarily result in reduced pathogenicity. In *Setosphaeria turcica, in vitro* osmotic stress reduces fungal growth but enhances pathogenicity (Liu et al., 2021). In *Fusarium oxysporum*, impairment of cellulose degradation enhances virulence but reduces growth and conidiation (Gámez-Arjona et al., 2022). Here, in line with the reduction in *C. austroafricana* growth under *in vitro* osmotic stress (Swart et al., 1992), we found that some genes associated with growth were downregulated under drought stress while genes related to fungal metabolism were upregulated. This is consistent with the initial increase in lesion length although the pathogen's growth could be negatively affected at later timepoints. Furthermore, while the pathogen could be vulnerable to drought, it may retain the ability to infect the now-susceptible host through altered strategies, at least under mild drought stress. For example, the upregulation of genes such as *FpHsp104* and MFS transporters could respectively protect the pathogen from abiotic stresses (Xia et al., 2021) and the host's defense responses (Chen et al., 2017; Vela-Corcía et al., 2019; Chen et al., 2021) enabling survival in the drought-stressed host environment.

Upon rewatering following combined stress, host transcriptomic changes highlighted alterations in the expression of key genes involved in some of the major biotic and abiotic stress response pathways possibly suggesting prioritization of stress response over carbohydrate storage and growth. We found transcriptomic evidence indicating that the JA/ET signalling pathways could have been induced under RDPI. This could be related to the central role of JA in regulating responses to stress combinations and coordinating defence and growth (Pascual et al., 2023; Sood, 2023). Our transcriptomic data also suggested that the ABA-dependent pathway was possibly activated under PI, while the ABA-independent pathway could have been induced under RDPI. A possible scenario for this is that rewatering may signal a reduction in ABA accumulation under RDPI (Correia et al., 2014), while ABA may play a role in defense under PI (Adie et al., 2007; García-Andrade et al., 2020). While these stress responses were activated, genes related to cell wall formation, including *EgrMYB46*, were uniquely downregulated during RDPI (Fig. 7d). Mutations in *AtMYB46* have been associated with increased resistance against necrotrophs (Ramírez et al., 2011). Consistent with the induction of the JA/ET signalling pathways, this suggests improved resistance to the pathogen during RDPI, and hence, indicates a trade-off between wood formation and stress response. However, we observed an increase in the expression of the carbon starvation-induced TF, *EgrNAC123* (Garapati et al., 2015; Ployet et al., 2019) under RDPI compared to PI (Fig. 7d), suggesting a possible shortage of resources largely caused by the pathogen attack. Thus, the canonical defense mechanisms were activated and resources were diverted towards defense, potentially leading to carbon starvation (Oliva et al., 2014) during RDPI due to multiple factors such as the available carbon pool, speed of recovery of photosynthesis, and exposure to subsequent stresses.

The changes in the pathogen transcriptome during rewatering indicate a reversal of some drought-induced changes and downregulation of some fungal metabolic pathways. Genes potentially encoding GT1 and GH72, upregulated during drought, were downregulated during rewatering indicating elastic responses. The downregulation of genes related to some fungal metabolic pathways may be related to the changes in the resistance responses of the host during rewatering. In support of this, the downregulation of the putative ortholog of MFS transporter, which exports SA in the pathogen (Chen et al., 2021), matches the downregulation of SA biosynthesis genes in the host (Fig. 7b). It could also be possible that the pathogen may take advantage of the changes in the host upon rewatering and may have contributed to carbon starvation in the plants (Oliva et al., 2014).

In summary, we showed that mild drought stress increased host susceptibility to *C. austroafricana* in a moderately resistant *E. grandis* genotype under combined stress and that this was possibly related to transcriptional rewiring involving the JA/ET, SA, and GA signalling pathways in the host as well as changes in the fungal transcriptome that could alter host-pathogen interaction. Upon rewatering, our transcriptomic data revealed prioritization of defense at the expense of cell wall formation and carbohydrate storage in the host and downregulation of some fungal metabolic processes indicating that the pathogen could take advantage of the changes in the host. Overall, the key molecular processes and genes we identified in both the host and the pathogen shed light on the complex molecular mechanisms underlying biotic stress responses under the cycles of exposure to and recovery from abiotic stresses such as drought in forest trees and contribute to devising mitigation strategies for tree health risks under a changing climate such as future tree breeding and use of beneficial microorganisms.

CRediT authorship contribution statement

Demissew Tesfaye Teshome: Writing – original draft, Methodology, Investigation, Formal analysis, Conceptualization. **Godfrey Elijah Zharare:** Writing – review & editing. **Raphael Ployet:** Writing – review & editing. **Sanushka Naidoo:** Writing – review & editing, Methodology, Funding acquisition, Conceptualization.

Declaration of competing interest

The authors declare that they have no known competing financial interests or personal relationships that could have appeared to influence the work reported in this paper.

Acknowledgements

This work was supported by the Technology Innovation Agency of South Africa, Woldia University, and the University of Pretoria. The authors thank Tanya Pretorius and Erik Visser for helping with data analysis and commenting the manuscript.

Supplementary materials

Supplementary material associated with this article can be found, in the online version, at doi:10.1016/j.stress.2024.100697.

Data availability

The data sets supporting the results of this manuscript are available on the National Centre for Biotechnology Information (NCBI) repository BioProject accession number PRJNA896601.

References

Adie, BA, Perez-Perez, J, Perez-Perez, MM, Godoy, M, Sanchez-Serrano, J-J, Schmelz, EA, Solano, R., 2007. ABA is an essential signal for plant resistance to pathogens affecting JA biosynthesis and the activation of defenses in *Arabidopsis*. Plant Cell 19 (5), 1665–1681.

Aguirre, NM, Ochoa, ME, Holmlund, HI, Palmeri, GN, Lancaster, ER, Gilderman, GS, Taylor, SR, Sauer, KE, Borges, AJ, Lamb, AN., 2024. How megadrought causes extensive mortality in a deep-rooted shrub species normally resistant to drought-induced dieback: The role of a biotic mortality agent. Plant Cell Environ. 47 (4), 1053–1069.

Amrutha, S, Muneera Parveen, AB, Muthupandi, M, Sivakumar, V, Nautiyal, R, Dasgupta, MG, 2019. Variation in morpho-physiological, biochemical and molecular responses of two Eucalyptus species under short-term water stress. Acta Bot. Croat. 78 (2), 125–134.

Backer, R, Naidoo, S, Van den Berg, N., 2019. The NONEXPRESSOR OF PATHOGENESIS-RELATED GENES 1 (NPR1) and related family: mechanistic insights in plant disease resistance. Front. Plant Sci. 10, 102.

Bhambra, GK, Wang, ZY, Soanes, DM, Wakley, GE, Talbot, NJ., 2006. Peroxisomal carnitine acetyl transferase is required for elaboration of penetration hyphae during plant infection by *Magnaporthe grisea*. Mol. Microbiol. 61 (1), 46–60.

Bostock, RM, Pye, MF, Roubtsova, TV., 2014. Predisposition in plant disease: exploiting the nexus in abiotic and biotic stress perception and response. Annu Rev. Phytopathol. 52, 517–549.

Brown, K, Takawira, LT, O'Neill, MM, Mizrachi, E, Myburg, AA, Hussey, SG, 2019. Identification and functional evaluation of accessible chromatin associated with wood formation in *Eucalyptus grandis*. New Phytol. 223 (4), 1937–1951.

Cao, FY, Yoshioka, K, Desveaux, D., 2011. The roles of ABA in plant–pathogen interactions. J. Plant Res. 124 (4), 489–499.

Chen, H, Hwang, JE, Lim, CJ, Kim, DY, Lee, SY, Lim, CO., 2010. *Arabidopsis DREB2C* functions as a transcriptional activator of *HsfA3* during the heat stress response. Biochem. Biophys. Res. Commun. 401 (2), 238–244.

Chen, L-H, Tsai, H-C, Yu, P-L, Chung, K-R., 2017. A major facilitator superfamily transporter-mediated resistance to oxidative stress and fungicides requires Yap1, Skn7, and MAP kinases in the citrus fungal pathogen *Alternaria alternata*. PLoS. One 12 (1), e0169103.

Chen, Q, Lei, L, Liu, C, Zhang, Y, Xu, Q, Zhu, J, Guo, Z, Wang, Y, Li, Q, Li, Y., 2021. Major facilitator superfamily transporter gene *FgMFS1* is essential for *Fusarium graminearum* to deal with salicylic acid stress and for its pathogenicity towards wheat. Int. J. Mol. Sci. 22 (16), 8497.

Choudhary, A, Senthil-Kumar, M., 2022. Drought attenuates plant defence against bacterial pathogens by suppressing the expression of *CBP60g/SARD1* during combined stress. Plant Cell Environ. 45 (4), 1127–1145.

Correia, B, Pintó-Marijuan, M, Castro, BB, Brossa, R, López-Carbonell, M, Pinto, G., 2014. Hormonal dynamics during recovery from drought in two *Eucalyptus globulus* genotypes: from root to leaf. Plant Physiol. Biochem. 82, 151–160.

da Silva, AC, de, Oliveira, Silva, FM, Milagre, JC, Omena-Garcia, RP, Abreu, MC, Mafia, RG, Nunes-Nesi, A, Alfenas, AC., 2018. Eucalypt plants are physiologically and metabolically affected by infection with *Ceratocystis fimbriata*. Plant Physiol. Biochem. 123, 170–179.

Du, Y, Hong, L, Tang, W, Li, L, Wang, X, Ma, H, Wang, Z, Zhang, H, Zheng, X, Zhang, Z., 2014. Threonine deaminase MoIlv1 is important for conidiogenesis and pathogenesis in the rice blast fungus *Magnaporthe oryzae*. Fungal Genet Biol. 73, 53–60.

Förster, S, Schmidt, LK, Kopic, E, Anschütz, U, Huang, S, Schlücking, K, Köster, P, Waadt, R, Larrieu, A, Batistič, O., 2019. Wounding-induced stomatal closure requires jasmonate-mediated activation of GORK K+ channels by a Ca2+ sensor-kinase CBL1-CIPK5 complex. Dev. Cell 48 (1), 87–99.

Free, SJ., 2013. Fungal cell wall organization and biosynthesis. Adv. Genet. 81, 33–82.

Gámez-Arjona, FM, Vitale, S, Voxeur, A, Dora, S, Müller, S, Sancho-Andrés, G, Montesinos, JC, Di Pietro, A, Sánchez-Rodríguez, C., 2022. Impairment of the cellulose degradation machinery enhances *Fusarium oxysporum* virulence but limits its reproductive fitness. Sci. Adv. 8 (16), eabl9734.

Garapati, P, Feil, R, Lunn, JE, Van Dijck, P, Balazadeh, S, Mueller-Roeber, B., 2015. Transcription factor *Arabidopsis* activating factor1 integrates carbon starvation responses with trehalose metabolism. Plant Physiol. 169 (1), 379–390.

García-Andrade, J, González, B, Gonzalez-Guzman, M, Rodriguez, PL, Vera, P., 2020. The role of ABA in plant immunity is mediated through the PYR1 receptor. Int. J. Mol. Sci. 21 (16), 5852.

Ghosh, SK, Slot, JC, Visser, EA, Naidoo, S, Sovic, MG, Conrad, AO, Kyre, B, Vijayakumar, V, Bonello, P., 2022. Mechanisms of Pine Disease Susceptibility Under Experimental Climate Change. Front. For. Glob. Change 5, 872584.

Gómez-Lim, MA, Valdés-López, V, Cruz-Hernandez, A, Saucedo-Arias, LJ, 1993. Isolation and characterization of a gene involved in ethylene biosynthesis from *Arabidopsis thaliana*. Gene 134 (2), 217–221.

Gomez-Gallego, M, Galiano, L, Martínez-Vilalta, J, Stenlid, J, Capador-Barreto, HD, Elfstrand, M, Camarero, JJ, Oliva, J., 2022. Interaction of drought-and pathogen-induced mortality in Norway spruce and Scots pine. Plant Cell Environ. 45 (8), 2292–2305.

Grille, S, Zaslawski, A, Thiele, S, Plat, J, Warnecke, D., 2010. The functions of steryl glycosides come to those who wait: Recent advances in plants, fungi, bacteria and animals. Prog. Lipid Res. 49 (3), 262–288.

Gryzenhout, M, Myburg, H, Van der Merwe, NA, Wingfield, BD, Wingfield, MJ., 2004. *Chrysoporthe*, a new genus to accommodate *Cryphonectria cubensis*. Stud. Mycol. 50, 119–142.

Gupta, A, Sarkar, AK, Senthil-Kumar, M., 2016. Global transcriptional analysis reveals unique and shared responses in *Arabidopsis thaliana* exposed to combined drought and pathogen stress. Front. Plant Sci. 7, 686.

Gupta, A, Senthil-Kumar, M., 2017. Transcriptome changes in *Arabidopsis thaliana* infected with *Pseudomonas syringae* during drought recovery. Sci. Rep. 7 (1), 9124.

Han, J, Zhou, Z., 2013. Dynamics of soil water evaporation during soil drying: laboratory experiment and numerical analysis. Sci. World J. 2013 (1), 240280.

Hoang, TV, Vo, KTX, Rahman, MM, Zhong, R, Lee, C, Ketudat Cairns, JR, Ye, Z-H, Jeon, J-S, 2023. SPOTTED-LEAF7 targets the gene encoding β-galactosidase9, which functions in rice growth and stress responses. Plant Physiol. 193 (2), 1109–1125.

Hussey, SG, Mizrachi, E, Creux, NM, Myburg, AA., 2013. Navigating the transcriptional roadmap regulating plant secondary cell wall deposition. Front. Plant Sci. 4, 325.

Illouz-Eliaz, N, Lande, K, Yu, J, Jow, B, Swift, J, Lee, T, Nobori, T, Castanon, RG, Nery, JR, Ecker, JR., 2023. Drought Recovery Induced Immunity Confers Pathogen Resistance. bioRxiv. 2023.2002. 2027.530256.

Kloth, KJ, Wiegers, GL, Busscher-Lange, J, van Haarst, JC, Kruijer, W, Bouwmeester, HJ, Dicke, M, Jongsma, MA., 2016. AtWRKY22 promotes susceptibility to aphids and modulates salicylic acid and jasmonic acid signalling. J. Exp. Bot. 67 (11), 3383–3396.

Klutts, JS, Yoneda, A, Reilly, MC, Bose, I, Doering, TL., 2006. Glycosyltransferases and their products: cryptococcal variations on fungal themes. FEMS. Yeast. Res. 6 (4), 499–512.

Ko, J-H, Jeon, H-W, Kim, W-C, Kim, J-Y, Han, K-H., 2014. The MYB46/MYB83-mediated transcriptional regulatory programme is a gatekeeper of secondary wall biosynthesis. Ann. Bot. 114 (6), 1099–1107.

Koizumi, N., 1996. Isolation and responses to stress of a gene that encodes a luminal binding protein in *Arabidopsis thaliana*. Plant and cell physiology 37 (6), 862–865.

Kramer, B, Thines, E, Foster, AJ., 2009. MAP kinase signalling pathway components and targets conserved between the distantly related plant pathogenic fungi *Mycosphaerella graminicola* and *Magnaporthe grisea*. Fungal Genetics Biol. 46 (9), 667–681.

Kuromori, T, Seo, M, Shinozaki, K., 2018. ABA transport and plant water stress responses. Trends. Plant Sci. 23 (6), 513–522.

Lan, Z, Krosse, S, Achard, P, van Dam, NM, Bede, JC., 2014. DELLA proteins modulate *Arabidopsis* defences induced in response to caterpillar herbivory. J. Exp. Bot. 65 (2), 571–583.

Langfelder, P, Horvath, S., 2008. WGCNA: an R package for weighted correlation network analysis. BMC. Bioinformatics. 9 (1), 1–13.

Langfelder, P, Luo, R, Oldham, MC, Horvath, S., 2011. Is my network module preserved and reproducible? PLoS. Comput. Biol. 7 (1), e1001057.

Li, C, Wang, K., 2003. Differences in drought responses of three contrasting *Eucalyptus microtheca* F. Muell. populations. For. Ecol. Manage 179 (1-3), 377–385.

Li, S, Han, X, Yang, L, Deng, X, Wu, H, Zhang, M, Liu, Y, Zhang, S, Xu, J., 2018. Mitogen-activated protein kinases and calcium-dependent protein kinases are involved in wounding-induced ethylene biosynthesis in *Arabidopsis thaliana*. Plant Cell Environ. 41 (1), 134–147.

Liang, Y, Xiong, W, Steinkellner, S, Feng, J., 2018. Deficiency of the melanin biosynthesis genes *SCD1* and *THR1* affects sclerotial development and vegetative growth, but not pathogenicity, in *Sclerotinia sclerotiorum*. Mol. Plant Pathol. 19 (6), 1444–1453.

Liu, Y, Gong, X, Li, M, Si, H, Zhou, Q, Liu, X, Fan, Y, Zhang, X, Han, J, Gu, S., 2021. Effect of osmotic stress on the growth, development and pathogenicity of *Setosphaeria turcica*. Front. Microbiol. 12, 706349.

Lockhart, DE, Stanley, M, Raimi, OG, Robinson, DA, Boldovjakova, D, Squair, DR, Ferenbach, AT, Fang, W, van Aalten, DM., 2020. Targeting a critical step in fungal hexosamine biosynthesis. J. Biol. Chem. 295 (26), 8678–8691.

Mangwanda, R, Myburg, AA, Naidoo, S., 2015. Transcriptome and hormone profiling reveals *Eucalyptus grandis* defence responses against *Chrysoporthe austroafricana*. BMC. Genomics. 16 (1), 1–13.

Mangwanda, R, Zwart, L, van der Merwe, NA, Moleleki, LN, Berger, DK, Myburg, AA, Naidoo, S., 2016. Localization and transcriptional responses of *Chrysoporthe austroafricana* in *Eucalyptus grandis* identify putative pathogenicity factors. Front. Microbiol. 7, 1953.

McGrath, KC, Dombrecht, B, Manners, JM, Schenk, PM, Edgar, CI, Maclean, DJ, Scheible, W-R, Udvardi, MK, Kazan, K., 2005. Repressor-and activator-type ethylene response factors functioning in jasmonate signaling and disease resistance identified via a genome-wide screen of *Arabidopsis* transcription factor gene expression. Plant Physiol. 139 (2), 949–959.

Mei, S, Zhang, M, Ye, J, Du, J, Jiang, Y, Hu, Y., 2023. Auxin contributes to jasmonate-mediated regulation of abscisic acid signaling during seed germination in *Arabidopsis*. Plant Cell 35 (3), 1110–1133.

Mittler, R., 2006. Abiotic stress, the field environment and stress combination. Trends. Plant Sci. 11 (1), 15–19.

Moretti, M, Rossi, M, Ciuffo, M, Turina, M., 2014. Functional characterization of the three mitogen-activated protein kinase kinases (MAP2Ks) present in the *Cryphonectria parasitica* genome reveals the necessity of Cpkk1 and Cpkk2, but not Cpkk3, for pathogenesis on chestnut (*Castanea* spp.). Mol. Plant Pathol. 15 (5), 500–512.

Murray, SL, Ingle, RA, Petersen, LN, Denby, KJ., 2007. Basal resistance against *Pseudomonas syringae* in *Arabidopsis* involves WRKY53 and a protein with homology to a nematode resistance protein. Mol. Plant Microbe Interact. 20 (11), 1431–1438.

Myburg, AA, Grattapaglia, D, Tuskan, GA, Hellsten, U, Hayes, RD, Grimwood, J, Jenkins, J, Lindquist, E, Tice, H, Bauer, D., 2014. The genome of *Eucalyptus grandis*. Nature 510 (7505), 356–362.

Naidoo, R, Ferreira, L, Berger, DK, Myburg, AA, Naidoo, S., 2013. The identification and differential expression of *Eucalyptus grandis* pathogenesis-related genes in response to salicylic acid and methyl jasmonate. Front. Plant Sci. 4, 42592.

Navarro, L, Bari, R, Achard, P, Lisón, P, Nemri, A, Harberd, NP, Jones, JD., 2008. DELLAs control plant immune responses by modulating the balance of jasmonic acid and salicylic acid signaling. Curr. Biol. 18 (9), 650–655.

Nguyen, HC, Cao, PB, San Clemente, H, Ployet, R, Mounet, F, Ladouce, N, Harvengt, L, Marque, C, Teulieres, C, 2017. Special trends in CBF and DREB2 groups in *Eucalyptus gunnii vs Eucalyptus grandis* suggest that CBF are master players in the trade-off between growth and stress resistance. Physiol. Plant 159 (4), 445–467.

Nguyen, QB, Kadotani, N, Kasahara, S, Tosa, Y, Mayama, S, Nakayashiki, H., 2008. Systematic functional analysis of calcium-signalling proteins in the genome of the rice-blast fungus, *Magnaporthe oryzae*, using a high-throughput RNA-silencing system. Mol. Microbiol. 68 (6), 1348–1365.

Oliva, J, Stenlid, J, Martínez-Vilalta, J., 2014. The effect of fungal pathogens on the water and carbon economy of trees: implications for drought-induced mortality. New Phytol. 203 (4), 1028–1035.

Pascual, LS, Mittler, R, Sinha, R, Peláez-Vico, MÁ, López-Climent, MF, Vives-Peris, V, Gómez-Cadenas, A, Zandalinas, SI., 2023. Jasmonic acid is required for tomato acclimation to multifactorial stress combination. Environ. Exp. Bot., 105425

Ployet, R, Veneziano Labate, MT, Regiani Cataldi, T, Christina, M, Morel, M, San Clemente, H, Denis, M, Favreau, B, Tomazello Filho, M, Laclau, JP, 2019. A systems biology view of wood formation in *Eucalyptus grandis* trees submitted to different potassium and water regimes. New Phytol. 223 (2), 766–782.

Prasch, CM, Sonnewald, U., 2013. Simultaneous application of heat, drought, and virus to *Arabidopsis* plants reveals significant shifts in signaling networks. Plant Physiol. 162 (4), 1849–1866.

Qi, Z, Liu, M, Dong, Y, Yang, J, Zhang, H, Zheng, X, Zhang, Z., 2016. Orotate phosphoribosyl transferase MoPyr5 is involved in uridine 5′-phosphate synthesis and pathogenesis of *Magnaporthe oryzae*. Appl. Microbiol. Biotechnol. 100, 3655–3666.

Rafiei, V, Vélëz, H, Tzelepis, G., 2021. The role of glycoside hydrolases in phytopathogenic fungi and oomycetes virulence. Int. J. Mol. Sci. 22 (17), 9359.

Ramírez, V, Agorio, A, Coego, A, García-Andrade, J, Hernández, MJ, Balaguer, B, Ouwerkerk, PB, Zarra, I, Vera, P., 2011. MYB46 modulates disease susceptibility to *Botrytis cinerea* in *Arabidopsis*. Plant Physiol. 155 (4), 1920–1935.

Robert-Seilaniantz, A, Grant, M, Jones, JD., 2011. Hormone crosstalk in plant disease and defense: more than just jasmonate-salicylate antagonism. Ann. Rev. Phytopathol. 49, 317–343.

Roux, J, Myburg, H, Wingfield, B, Wingfield, M., 2003. Biological and phylogenetic analyses suggest that two *Cryphonectria* spp. cause cankers of *Eucalyptus* in Africa. Plant Dis. 87 (11), 1329–1332.

Santos, B, Pinto, G, Berenguer, H, Correia, B, Amaral, J, Gómez-Cadenas, A, Alves, A., 2024. Physiological and hormonal responses of drought-stressed *Eucalyptus* seedlings infected with *Neofusicoccum kwambonambiense*. Plant Pathol. 73, 810–823.

Sarmiento-Villamil, JL, Prieto, P, Klosterman, SJ, García-Pedrajas, MD., 2018. Characterization of two homeodomain transcription factors with critical but distinct roles in virulence in the vascular pathogen *Verticillium dahliae*. Mol. Plant Pathol. 19 (4), 986–1004.

Schomburg, FM, Bizzell, CM, Lee, DJ, Zeevaart, JA, Amasino, RM., 2003. Overexpression of a novel class of gibberellin 2-oxidases decreases gibberellin levels and creates dwarf plants. Plant Cell 15 (1), 151–163.

Segers, G, Bradshaw, N, Archer, D, Blissett, K, Oliver, R., 2001. Alcohol oxidase is a novel pathogenicity factor for *Cladosporium fulvum*, but aldehyde dehydrogenase is dispensable. Mol. Plant-Microbe Interact. 14 (3), 367–377.

Son, H, Seo, Y-S, Min, K, Park, AR, Lee, J, Jin, J-M, Lin, Y, Cao, P, Hong, S-Y, Kim, E-K, 2011. A phenome-based functional analysis of transcription factors in the cereal head blight fungus, *Fusarium graminearum*. PLoS. Pathog. 7 (10), e1002310.

Sood, M., 2023. Jasmonates:"The Master Switch" for Regulation of Developmental and Stress Responses in Plants. J. Plant Growth Regul. 42 (8), 5247–5265.

Sözen, C, Schenk, ST, Boudsocq, M, Chardin, C, Almeida-Trapp, M, Krapp, A, Hirt, H, Mithöfer, A, Colcombet, J., 2020. Wounding and insect feeding trigger two independent MAPK pathways with distinct regulation and kinetics. Plant Cell 32 (6), 1988–2003.

Susiluoto, S, Berninger, F., 2007. Interactions between morphological and physiological drought responses in *Eucalyptus microtheca*. Silva Fennica 41 (2), 221.

Suzuki, N, Rivero, RM, Shulaev, V, Blumwald, E, Mittler, R., 2014. Abiotic and biotic stress combinations. New Phytol. 203 (1), 32–43.

Swart, W, Conradie, E, Wingfield, M., 1992. Effects of water stress on the development of cambial lesions caused by *Cryphonectria cubensis* on *Eucalyptus grandis*. Plant Dis. 76 (7), 744–746.

Sweigard, JA, Carroll, AM, Farrall, L, Chumley, FG, Valent, B., 1998. *Magnaporthe grisea* pathogenicity genes obtained through insertional mutagenesis. Mol. Plant-Microbe Inter. 11 (5), 404–412.

Tateda, C, Watanabe, K, Kusano, T, Takahashi, Y., 2011. Molecular and genetic characterization of the gene family encoding the voltage-dependent anion channel in *Arabidopsis*. J. Exp. Bot. 62 (14), 4773–4785.

Teshome, DT, Zharare, GE, Naidoo, S., 2020. The threat of the combined effect of biotic and abiotic stress factors in forestry under a changing climate. Front. Plant Sci. 11, 1874.

Teshome, DT, Zharare, GE, Ployet, R, Naidoo, S., 2023. Transcriptional reprogramming during recovery from drought stress in *Eucalyptus grandis*. Tree Physiol. 43 (6), 979–994.

Urban, M, Cuzick, A, Seager, J, Wood, V, Rutherford, K, Venkatesh, SY, Sahu, J, Iyer, SV, Khamari, L, De Silva, N., 2022. PHI-base in 2022: A multi-species phenotype database for Pathogen–Host Interactions. Nucleic Acids Res. 50 (D1), D837–D847.

Van Heerden, S, Amerson, H, Preisig, O, Wingfield, B, Wingfield, M., 2005. Relative pathogenicity of *Cryphonectria cubensis* on *Eucalyptus* clones differing in their resistance to *C. cubensis*. Plant Dis. 89 (6), 659–662.

Vela-Corcía, D, Aditya Srivastava, D, Dafa-Berger, A, Rotem, N, Barda, O, Levy, M, 2019. MFS transporter from *Botrytis cinerea* provides tolerance to glucosinolate-breakdown products and is required for pathogenicity. Nature Commun. 10 (1), 2886.

Webb, K, Ona, I, Bai, J, Garrett, K, Mew, T, Vera Cruz, C, Leach, J, 2010. A benefit of high temperature: increased effectiveness of a rice bacterial blight disease resistance gene. New Phytolo. 185 (2), 568–576.

Wingfield, BD, Ades, PK, FA, Al-Naemi, Beirn, LA, Bihon, W, Crouch, JA, De Beer, ZW, De Vos, L, Duong, TA, Fields, CJ., 2015. Draft genome sequences of *Chrysoporthe austroafricana, Diplodia scrobiculata, Fusarium nygamai, Leptographium lundbergii, Limonomyces culmigenus, Stagonosporopsis tanaceti*, and *Thielaviopsis punctulata*. IMa Fungus. 6 (1), 233–248.

Wingfield, M., 1989. First record of *Cryphonectria* canker of *Eucalyptus* in South Africa. Phytophylactica 21, 311–313.

Wiszniewski, AA, Zhou, W, Smith, SM, Bussell, JD., 2009. Identification of two *Arabidopsis* genes encoding a peroxisomal oxidoreductase-like protein and an acyl-CoA synthetase-like protein that are required for responses to pro-auxins. Plant Mol. Biol. 69, 503–515.

Xia, H, Chen, L, Fan, Z, Peng, M, Zhao, J, Chen, W, Li, H, Shi, Y, Ding, S, Li, H, 2021. Heat stress tolerance gene *FpHsp104* affects conidiation and pathogenicity of *Fusarium pseudograminearum*. Front. Microbiol. 12, 695535.

Yao, GQ, Li, FP, Nie, ZF, Bi, MH, Jiang, H, Liu, XD, Wei, Y, Fang, XW., 2021. Ethylene, not ABA, is closely linked to the recovery of gas exchange after drought in four Caragana species. Plant Cell Environ. 44 (2), 399–411.

Yin, Y, Mao, X, Yang, J, Chen, X, Mao, F, Xu, Y., 2012. dbCAN: a web resource for automated carbohydrate-active enzyme annotation. Nucleic Acids Res. 40 (W1), W445–W451.

Yoshida, T, Fujita, Y, Sayama, H, Kidokoro, S, Maruyama, K, Mizoi, J, Shinozaki, K, Yamaguchi-Shinozaki, K., 2010. AREB1, AREB2, and ABF3 are master transcription factors that cooperatively regulate ABRE-dependent ABA signaling involved in drought stress tolerance and require ABA for full activation. Plant J. 61 (4), 672–685.

Yoshida, T, Mogami, J, Yamaguchi-Shinozaki, K., 2014. ABA-dependent and ABA-independent signaling in response to osmotic stress in plants. Curr. Opinion Plant Biol. 21, 133–139.

Yuan, Q, Yan, Y, Sohail, MA, Liu, H, Huang, J, Hsiang, T, Zheng, L., 2021. A novel hexose transporter ChHxt6 is required for hexose uptake and virulence in *Colletotrichum higginsianum*. Int. J. Mol. Sci. 22 (11), 5963.

Zarattini, M, Farjad, M, Launay, A, Cannella, D, Soulié, M-C, Bernacchia, G, Fagard, M., 2021. Every cloud has a silver lining: how abiotic stresses affect gene expression in plant-pathogen interactions. J. Exp. Bot. 72 (4), 1020–1033.

Zhang, Z-L, Ogawa, M, Fleet, CM, Zentella, R, Hu, J, Heo, J-O, Lim, J, Kamiya, Y, Yamaguchi, S, Sun, T-p., 2011. Scarecrow-like 3 promotes gibberellin signaling by antagonizing master growth repressor DELLA in *Arabidopsis*. Proc. Natl. Acad. Sci. 108 (5), 2160–2165.

Zhong, R, Lee, C, Haghighat, M, Ye, ZH., 2021. Xylem vessel-specific SND5 and its homologs regulate secondary wall biosynthesis through activating secondary wall NAC binding elements. New Phytologist 231 (4), 1496–1509.

Zwart, L, Berger, DK, Moleleki, LN, Van Der Merwe, NA, Myburg, AA, Naidoo, S., 2017. Evidence for salicylic acid signalling and histological changes in the defence response of *Eucalyptus grandis* to *Chrysoporthe austroafricana*. Sci. Rep. 7, 45402.